

A Study of 5p Excitation in Atomic Barium I. The 5p Absorption Spectra of Ba I, Cs I and Related Elements

J. P. Connerade, M. W. D. Mansfield, G. H. Newsom, D. H. Tracy, M. A. Baig and K. Thimm

Phil. Trans. R. Soc. Lond. A 1979 **290**, 327-352

doi: 10.1098/rsta.1979.0002

Email alerting service

Receive free email alerts when new articles cite this article - sign up in the box at the top right-hand corner of the article or click [here](#)

To subscribe to *Phil. Trans. R. Soc. Lond. A* go to: <http://rsta.royalsocietypublishing.org/subscriptions>

A STUDY OF $5p$ EXCITATION IN ATOMIC BARIUM

I. THE $5p$ ABSORPTION SPECTRA OF Ba I, Cs I AND RELATED ELEMENTS

BY J. P. CONNERADE,* M. W. D. MANSFIELD,*§ G. H. NEWSOM,*†
D. H. TRACY,*|| M. A. BAIG* AND K. THIMM‡

* *Blackett Laboratory, Imperial College, London SW7 2AZ, U.K., and Physikalisches Institut, Universität Bonn, 53 Bonn, West Germany, and ‡ Physikalisches Institut, Universität Bonn, 53 Bonn, West Germany*

(Communicated by W. R. S. Garton, F.R.S. – Received 6 April 1978)

[Plates 1 and 2]

CONTENTS

	PAGE		PAGE
1. INTRODUCTION	327	4. CONCLUSION	351
2. EXPERIMENTAL	328	REFERENCES	351
3. RESULTS AND DISCUSSION	328		

New observations of the $5p$ spectra of Cs I and Ba I are reported. The extreme complexity of the structure does not permit precise configuration labels to be attached to all the excited levels. Nevertheless, more than 160 transitions in Ba I have been ordered into 14 series converging on experimentally known levels of the parent ion. An attempt has been made to analyse the limit structure by comparison with the data for Cs I and Hartree–Fock atomic structure calculations. The results obtained are consistent with previous interpretations of the double ionization anomaly in Ba I. Further comments are made on the comparison between experiment and the predictions of the r.p.a.e. theory for $5p$ excitation in Ba I. It is shown that the $5p^6 6s^2 S_{\frac{1}{2}} \rightarrow 5p^5 6s^2 P_{\frac{1}{2}}$ and $^2P_{\frac{3}{2}}$ transitions of Cs I have been incorrectly identified and new assignments are proposed.

1. INTRODUCTION

Many papers have recently been devoted to excited core spectra of Ba I since the publication of Wendin's (1973 *a, b*) theoretical predictions (Ederer *et al.* 1974, 1975, Rabe *et al.* 1974, Connerade *et al.* 1974, Connerade & Mansfield 1974, Fliflet *et al.* 1974, Hansen *et al.* 1975, Fliflet *et al.* 1975, Wendin 1976, etc., for 4d vacancies; Hansen 1974, 1975, Hansen *et al.* 1975, Ederer *et al.* 1974, Connerade *et al.* 1974, Reader & Epstein 1974, Connerade & Tracy 1977, etc., for $5p$ vacancies).

Much of the work on neutral atoms has been motivated by the desire to test the r.p.a.e. (random phase approximation with exchange) theory in what seemed initially an unambiguous case in view of the large difference which had been reported between the one-electron model and the

† Present address: Ohio State University, Columbus, Ohio, U.S.A. § Present address: U.K.A.E.A. Culham Laboratory, Abingdon, Oxon, England. || Present address: University of Wisconsin, Madison, Wisconsin, U.S.A.

full many-body treatment. Recent controversy on identifications (Ederer *et al.* 1975; Hansen *et al.* 1975; Fliflet *et al.* 1975; Wendin 1976) has perhaps led the discussion away from the original question, namely comparisons between predictions of the r.p.a.e., m.b.p.t. (many-body perturbation theory) or one-electron theories and experiment for the spectral distribution of oscillator strength.

Regarding 5p subshell excitation (Ederer *et al.* 1974; Connerade *et al.* 1974), the difficulty of relating observations to the r.p.a.e. predictions (Wendin 1973*b*) has been commented on by Connerade & Tracy (1977) in general terms and there has also been a number of papers on the anomalous double ionization rates (Hansen 1975 and references therein). Attempts at understanding the detailed structure have mainly relied on non-relativistic Hartree–Fock calculations and are hampered by the complex s–d mixing in the spectra of Cs, Ba and La.

Considerable progress has however been achieved (Reader 1976) in unravelling s–d mixing semi-empirically for the energy levels of Cs II as well as Ba III and La IV (Reader & Epstein 1975; Hellentin 1976), in the light of which tentative identifications for Cs I (Connerade 1970*a*) require revision.

The object of the present paper is to present in greater detail our data on Ba I and Cs I and to emphasize the importance of comparisons with observed spectra of other related elements, in particular Yb I (Tracy 1977).

2. EXPERIMENTAL

The absorption spectra of Cs I and Ba I were recorded at the 500 MeV synchrotron of the University of Bonn using experimental techniques which have already been fully described (Connerade *et al.* 1974, 1976). In addition, the Ba I absorption spectrum was observed at Imperial College, by means of a system similar to the one described by Garton *et al.* (1969) which provided a spectrum calibrated against internal wavelength standards and allowed the superposition of standards in the synchrotron experiments to be checked. A similar check for Cs I was made against Connerade's (1970*a*) measurements.

We have also had access to data on the 5p spectra of Sm I–Yb I reported by Tracy (1977) and to data on La I and Pr I (Connerade *et al.*, to be published) all of which have been obtained in Bonn with the same optical systems as our Cs I and Ba I spectra.

3. RESULTS AND DISCUSSION

The 5p absorption spectra of Cs I and Ba I are illustrated in figures 1 and 2. The surprising complexity of the 5p-hole spectrum of Cs I was first discovered by Beutler & Guggenheimer (1934) who were unable to account for the profusion of the observed structure using the one-electron model

$$5p^6 6s^2 S_{\frac{1}{2}} \rightarrow 5p^5 6s ({}^1, {}^3P) ns, nd. \quad (1)$$

Connerade (1970*a*) extended Beutler's observations, adding yet further to the complexity of the spectrum, using a spectrograph of six times the dispersion and a greater absorption path length.

Connerade (1970*a*) also suggested that a breakdown in the characterization of some of the $5p^5 6s$ levels could account for the failure of the simple one-electron model (1) and that a more correct excitation scheme would be

$$5p^6 6s^2 S_{\frac{1}{2}} \rightarrow (5p^5 6s \times 5p^5 5d) ns, nd, \quad (2)$$

which takes account of configuration mixing in the parent ion. A similar situation was found to exist in Rb I (Connerade 1970*b*) and subsequent observations of Rb I and K I (Mansfield 1973, 1975) confirmed the validity of Connerade's (1970*a, b*) approach for the heavier alkali spectra, although the detailed assignments are revised, in particular for the low-lying levels (Mansfield 1978). In the light of the more recent investigations, it is interesting that Beutler & Guggenheimer (1934) considered the possibility of relating the observed Cs I spectrum to the observed level structure of $5p^5 6s$ and $5p^5 5d$, although, as they commented, they were unable to find any theoretical justification for so doing.

The analysis of the Cs I and related spectra is thus critically dependent on what $5p^5 6s$ and $5p^5 5d$ levels are included in (2). Unfortunately, the early work on the parent ion configurations used by Connerade (1970*a, b*) in his analysis is very unreliable and the more recent work cited in the introduction has led to a substantial revision of the spark spectra. We attempt below to relate the more recent work on the spark spectra of Cs and Ba (Reader & Epstein 1975; Reader 1976; Hellentin 1976) to the present observations of the 5p spectrum of Ba I. We consider only the gross features of the Cs I spectrum: extensive new data between 400 and 600 Å requires detailed analysis and will be published at a later date. (1 Å = 0.1 nm = 10^{-10} m.)

Two further conclusions were drawn by Connerade (1970*a*) from his observations on alkali spectra, namely:

(A) That it is possible to distinguish between two kinds of double excitation:

Type 1. Double excitations which arise solely from mixing between two configurations of the same parity in the parent ion. As the mixing is always present (i.e. for all n values of the jumping electron in the spectrum of the neutral atom), the mixing gives rise to well-developed series converging on supernumerary limits. When the mixing in the limit system is severe, 'pure' one-electron transitions can no longer be defined and the supernumerary limits should be included in the main excitation scheme. The one-electron Δl selection rule for the running electron is not violated, as the effect is due only to the limits. Mansfield & Newsom (1977) have shown that the *lowest* members of Rydberg series are not generally of type 1.

Type 2. Double excitations which are due to mixing induced by the jumping electron (e.g. if the parent ion configurations have different parities). Since we assume there is no mixing between the corresponding configurations in the spark spectrum, the double excitation arises by virtue of coupling with the running electron, and the one-electron Δl selection rule can be violated for this electron. Long series do not necessarily arise for type 2 transitions, and they are much affected by the proximity of single excitations. Type 2 transitions are often weak and may be then considered separately from the main excitation scheme.

It is of course possible to imagine double excitations which arise through a combination of both mechanisms but the experimental distinction is not quite so clear. More recently, Süzer *et al.* (1976) have considered correlation satellites in atomic photoelectron spectra and have suggested that they could arise through initial state configuration interaction (i.s.c.i.), final ionic state configuration (f.i.s.c.i.) or continuum state configuration interaction (c.s.c.i.).

Although the final states in photoelectron spectroscopy are different from those involved in photoabsorption, f.i.s.c.i. is related to the type 1 process of Connerade (1970*a*). The process described as i.s.c.i. is specific to the neutral atom and would therefore lead to transitions in a third category (not considered by Connerade 1970*a*), where the double excitation arises independently of mixing in the excited state. For further discussion of the classification of Süzer *et al.* (1976), we refer the reader to a paper by Mansfield & Connerade (1978).

(B) In spectra which are dominated by type 1 transitions, we expect that the observed spectrum can be broadly divided into three regions: in the first, at longer wavelengths, lines are intense and well separated (i.e. are the first members of strong series); in the second, at intermediate wavelengths, there are many closely spaced lines where the series to many different limits overlap and in the third, at short wavelengths, where fewer limits are present, recognizable series emerge.

Connerade's (1970*a*) broad characterization of core-excited alkali spectra has since been verified experimentally for K I, Rb I (Mansfield 1973, 1975) and Ba II (Roig 1976). A case where the spread in parent ion energy splittings is smaller than the difference in energy between successive members of a Rydberg series has also been found (Mansfield & Connerade 1975).

The spectra of Ba I and Cs I are clearly dominated by transitions of type 1 (above) and the consequent division into three regions is illustrated in figures 1 and 2.

We have attempted to analyse the Ba I absorption spectrum by three distinct but complementary approaches, the combined use of which enables some progress to be made in unravelling the complex overlapping structures. The approaches are:

(i) Correlations with Roig's (1976) observations of the Ba⁺ absorption spectrum. Many strong lines in the Ba⁺ absorption spectrum are transitions to levels which serve as series limits in the absorption spectrum of the neutral atom. Roig's (1976) table of experimental energies for Ba⁺ therefore enables a number of transitions in neutral Ba to be ordered into unambiguous series. Unfortunately, detailed assignments for Ba⁺ do not exist, and one must therefore supplement this approach by comparisons of the limit structure with other spectra and with *ab initio* calculations. In the Ba I excitation scheme,

$$5p^6 6s^2 1S_0 \rightarrow 5p^5(6s \times 5d)^2 ns, nd \quad (J = 1),$$

series limits with $J = \frac{1}{2}, \frac{3}{2}$ are the only ones which can give rise to strong series, because the mixing in of supernumerary limits originates from $5p^5 6s^2 P_{\frac{1}{2}, \frac{3}{2}}$. Thus, the Ba⁺ transitions

$$5p^6 6s^2 S_{\frac{1}{2}} \rightarrow 5p^5(6s \times 5d)^2 \quad (J = \frac{1}{2}, \frac{3}{2})$$

should involve all the relevant upper levels (this is also true for any $5p^5 6p^2$ or $5p^5 4f^2$ levels which might appear). Unfortunately, Roig's (1976) spectrum also contains transitions from the metastable $5d^2 D$ level of Ba⁺ as well as excitations to higher configurations than (ii), which is a limitation in this approach.

(ii) Comparisons with $5p$ spectra of the lanthanides. This approach uses the fact that the importance of $6s$ – $5d$ mixing decreases progressively as one moves from Cs to Yb (Connerade & Tracy 1977), so that the Yb I $5p$ spectrum (Tracy 1977) is much simpler in overall structure than the $5p$ spectrum of Ba I. Since Yb I differs from Ba I essentially by a filled $4f$ subshell, one can argue that the Yb I spectrum reveals the hypothetical form of the Ba I spectrum in absence of $6s$ – $5d$ mixing. If one further assumes (as suggested in figure 3, plate 1) that it is possible to work back from Yb to Ba, then the Yb I assignments provide valuable information for the interpretation of Ba I and also Cs I.

(iii) Finally, one can resort to Hartree–Fock calculations and/or to the diagonalization of energy matrices with appropriately scaled Slater integrals, an approach which can often be of great value in the interpretation of inner shell spectra. The limitation here is the extent to which configuration mixing can be included in a realistic way. Thus, $5p^5 6s$ and $5p^5 5d$ have been treated by such methods (cf. Reader (1976) for Cs II), but the additional mixing which results from

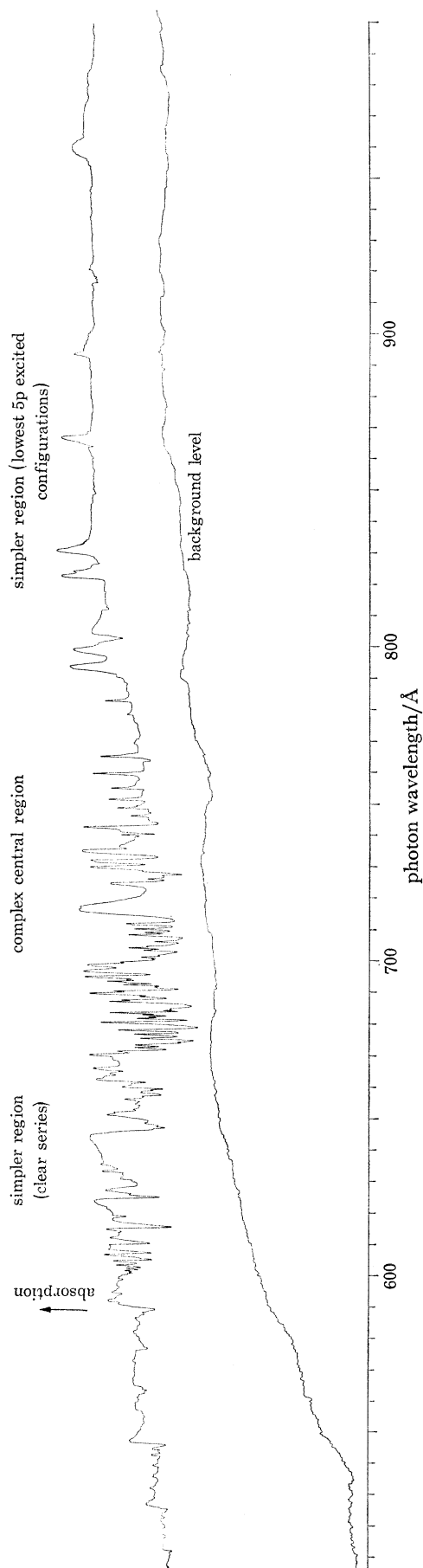


FIGURE 1. The absorption spectrum of Cs I between 560 and 1050 Å due to excitation of the 5p subshell. The division into regions of differing complexity follows Conneradé's (1970*a, b*) suggestion.

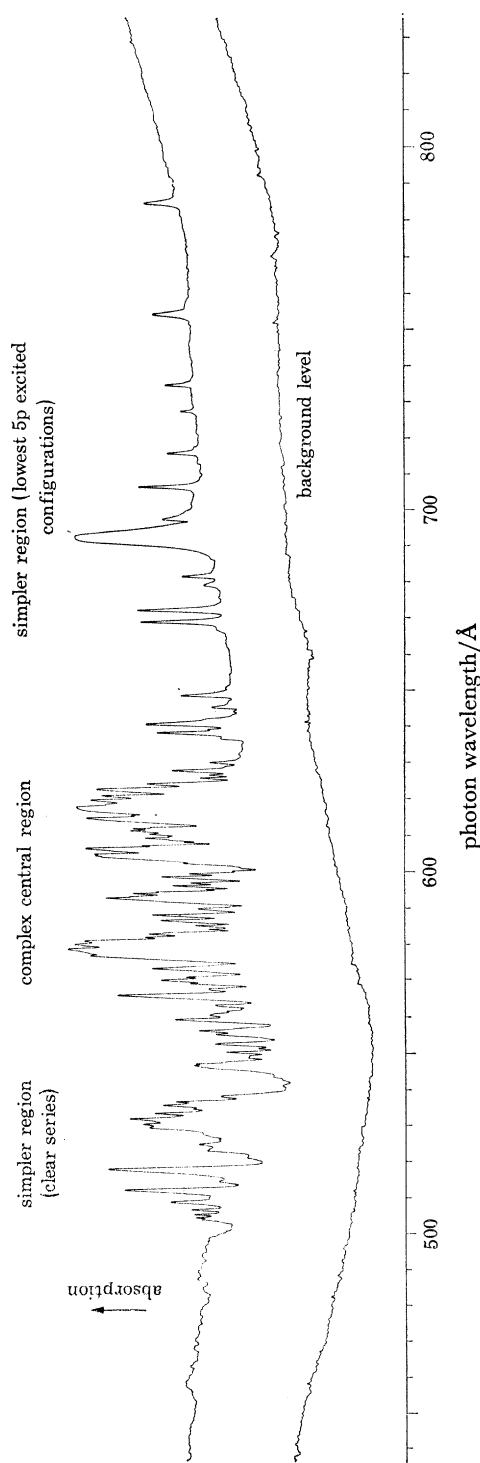


FIGURE 2. The absorption spectrum of Ba I between 440 and 830 Å due to excitation of the 5p subshell. The division into regions of differing complexity follows Conneradé's (1970*a, b*) suggestion.

coupling a *second* 6s or 5d electron is more difficult to calculate. Hansen (1975) has reported a non-relativistic treatment for $5p^5 5d 6s$ of Ba II and stresses the importance of including configuration mixing with $p^5 l^2$ ($l = s, p'$ and d) in the calculation. We have performed intermediate coupling calculations without configuration mixing using Hartree–Fock parameters for $5p^5 6s^2$, $5p^5 5d 6s$, $5p^5 6s 7s$, $5p^5 5d^2$ and other $5p$ -excited configurations in Ba II, Cs I and lanthanide elements. For the case reported by Hansen (1975) in Ba II we find, perhaps surprisingly, that configuration mixing produces fairly small shifts in energy, but the comparison with experiment for Ba I and Cs I reveals that the calculations are inadequate, in contrast with the situation for K I (Mansfield 1975) and Rb I (Mansfield 1978) where quite good agreement has been obtained. We feel that, while such calculations may indicate trends (e.g. Z -dependence) in a qualitative way, their accuracy is not sufficient to enable assignments around $Z = 56$. Rather, we have used them to estimate the energies of the most important $5p$ -excited configurations (see table 3).

Approach (i)

Approach (i) involved ordering the observed Ba I transitions into series using values of effective quantum number deduced from the parent ion structure and also taking account of the course of intensities. The remarkable fact is that nearly all the observed transitions in Ba I can be arranged into a comparatively small number of series, running to experimentally established limits. In table 1 (*a–l*) we list the transitions by series and, in figure 4, plate 2, we show how the ordering has been accomplished.

For a number of transitions, merely computing effective quantum numbers remains an ambiguous procedure as many of the series exhibit irregularities due to mutual perturbations. We have therefore resorted to the graphical techniques of multi-channel quantum defect theory (Lu & Fano 1970), which, even in the simplified ‘many-channel two-limit’ approach used here, have the advantage of including effects due to perturbations between channels.

TABLE 1. $5p$ SUBSHELL EXCITATION SERIES IN Ba I

(a) Series to 199662 cm^{-1} limit (634.40 \AA , Roig 1976)

no.	$\lambda/\text{\AA}$	ν/cm^{-1}	n^*
1	(576.11)*	(173578)*	(2.05)*
2	531.47	188157	3.08
3	517.58	193207	4.12
4	511.44	195528	5.15
5	508.18	196779	6.17
6	506.28	197520	7.16
7	505.02	198013	8.16
8	504.07	198386	9.27
9	503.48	198617	10.25
10	502.89	198852	11.64
11	502.27	199096	13.92

This series is tentatively assigned as

$$5p^6 6s^2 1S_0 \rightarrow 5p^5 6s^2 ({}^2P_{\frac{3}{2}}) nd [{}^{\frac{3}{2}}]_1,$$

the first member of which is

$$5p^6 6s^2 1S_0 \rightarrow 5p^5 6s^2 ({}^2P_{\frac{3}{2}}) 5d 1P_1.$$

The lines are very broad and intense (see figures 2 and 4). Small changes in the series limit derived from Roig's (1976) observations do not significantly improve the course of quantum defects. A plot of ν_a (quantum defect, modulo 1) against energy for this series is given in figure 5 (*a*).

* The association of lowest series members is *tentative* (see text) and the comparisons given in table 5 (*a–c*) should also be consulted.

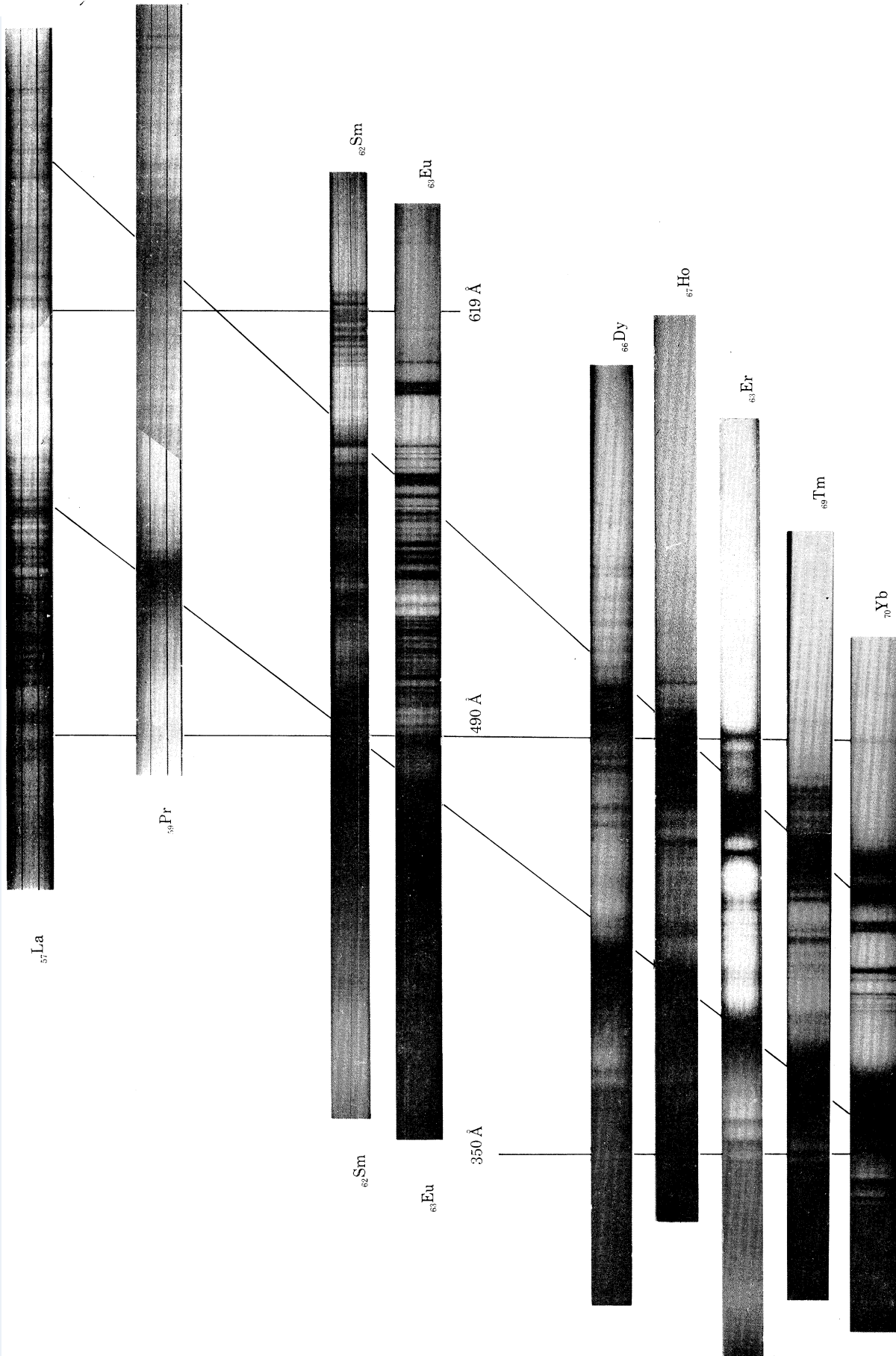


FIGURE 3. The 5p absorption spectra of the elements La I–Yb I recorded at the 500 MeV synchrotron in Bonn. The spectra of Sm I–Yb I have been reported by Tracy (1977) and work on La I–Pr I is still in progress. Note the persistence of the 1P_1 – 3P limit structure from Yb back to Pr I. Around La I ($6s \times 5d$) mixing begins to complicate this pattern.

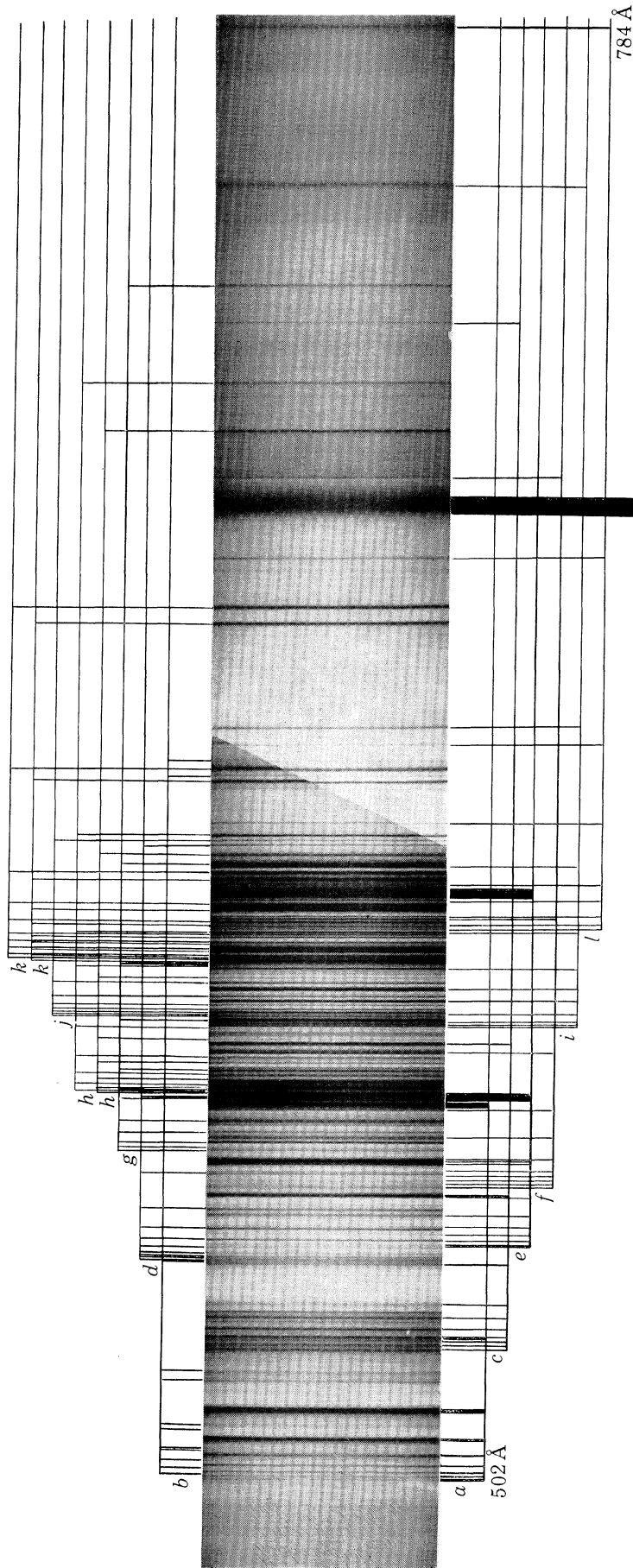


FIGURE 4. The 5p absorption spectrum of Ba I, showing how the ordering into 14 channels is accomplished (see text). The labels refer to tables 1 (a-l) and figure 6.

TABLE 1 (cont.)

(b) Series to 199 662 cm⁻¹ limit (634.40 Å, Roig 1976)

no.	$\lambda/\text{Å}$	ν/cm^{-1}	n^*
1	(642.41)	(155 664)	(1.58)
	(639.45)	(156 384)	(1.59)
2	546.46	182 998	2.57
	545.42	183 346	2.59
3	523.77	190 925	3.54
	522.74	191 298	3.62
4	514.13	194 504	4.61
	513.60	194 703	4.70
5	509.52	196 263	5.68
6	507.14	197 183	6.65
7	505.65	197 766	7.61

These series consist of weak sharp lines. If they are interpreted as ns series, the most likely explanation would seem that they converge on nearly coincident limits with $J = \frac{1}{2}$, i.e. that the series are

$$5p^6 6s^2 {}^1S_0 \rightarrow (5p^5 6s^2 {}^2P_{\frac{1}{2}}) ns[\frac{1}{2}]_1,$$

and

$$5p^6 6s^2 {}^1S_0 \rightarrow (5p^5 5d^2 {}^2P_{\frac{1}{2}}) ns[\frac{1}{2}]_1,$$

which is not inconsistent with the Hartree–Fock estimates of table 3 (f).

A plot of ν_b (quantum defect, modulo 1) against energy for this series is given in figure 5(b).

(c) Series to 189 669 cm⁻¹ (near 677.27 Å, Roig 1976)

no.	$\lambda/\text{Å}$	ν/cm^{-1}	n^*
1	(727.40)	(137 476)	(1.45)
2	588.26	169 993	2.36
3	556.85	179 582	3.30
4	543.92	183 851	4.34
5	537.84	185 928	5.40
6	535.22	186 839	6.21
7	532.95	187 635	7.32
8	531.69	188 080	8.27
9	530.77	188 404	9.26
10	530.08	188 649	10.30
11	529.62	188 816	11.24

This is a weak sharp series. A two-dimensional Lu–Fano graph, plotted against $\nu_{a,b}$ yields an approximate straight line (see figure 5c), with a suggested perturbation by the 2nd member of channel a . The first member of the series lies off the curve, as is found in many series (Lu & Fano 1970).

(d) Series to 183 844 cm⁻¹ limit (705.16 Å, Roig 1976)

no.	$\lambda/\text{Å}$	ν/cm^{-1}	n^*
1	(622.94)	(160 529)	(2.17)
2	577.08	173 285	3.22
3	562.81	177 680	4.22
4	556.03	179 847	5.24
5	552.29	181 063	6.28
6	550.15	181 770	7.27
7	548.68	182 255	8.31
8	547.72	182 575	9.30
9	546.99	182 817	10.33
10	546.46	182 998	11.39
11	546.07	183 128	12.38
12	545.77	183 227	13.33
13	545.42	183 346	14.84

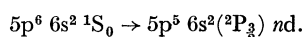
Fairly strong, sharp series. The four lowest members of channel b lie below 183 844 cm⁻¹ and a two-dimensional Lu–Fano plot (figure 5d) indicates that they are the main perturbers of series d . Hartree–Fock calculations (figure 6) suggest that the present series, which seem to involve the excitation of an nd electron, should be assigned

$$5p^6 6s^2 {}^1S_0 \rightarrow \{(5p^5 5d {}^3D) 6s {}^2D_{\frac{3}{2}}\} nd.$$

TABLE 1 (*cont.*)(e) Series to 182993 cm⁻¹ limit (709.42 Å, Roig 1976)

no.	$\lambda/\text{Å}$	ν/cm^{-1}	n^*
1	(617.80)	(161864)	(2.28)
2	579.37	172600	3.25
3	565.15	176944	4.26
4	558.53	179040	5.27
5	555.03	180172	6.24
6	552.74	180917	7.27
7	551.39	181361	8.20
8	550.15	181770	9.47
9	549.35	182033	10.70

Series *e* consists of fairly intense, broad transition and is probably due to the excitation of an *nd* electron. A two-dimensional Lu-Fano plot against channel *a* does not reveal any significant mutual perturbation. The proximity in energy of two intense transitions from channel *b* (at 182998 and 183346 cm⁻¹) to the series limit (at 182993 cm⁻¹) might affect 8 and 9 (see figure 5*e*). This conclusion must be treated with caution because 181770 cm⁻¹ is common to series *e* and *d*. Calculations suggest the assignment



The lower levels in this series perturb channel *f*.

(f) Series to 179245 cm⁻¹ (near 728.66 Å, Roig 1976)

no.	$\lambda/\text{Å}$	ν/cm^{-1}	n^*
1	(697.30)	(143411)	(1.75)
2	611.93	163416	2.63
3	586.13	170610	3.57
4	575.27	173831	4.51
5	569.66	175542	5.44
6	566.32	176577	6.41
7	—	—	—
8	562.39	177813	8.75
9	561.57	178071	9.67
10	560.95	178270	10.61
11	560.36	178453	11.77
12	559.99	178573	12.77

This series is weak and sharp and may be due to the excitation of an *ns* electron. The third member of series *e* at 565.15 Å falls between the 6th and 8th member and is responsible for the perturbation shown in figure 5(*f*). Our calculations of the limit structure are not sufficiently accurate to establish any identification of this series.

(g) Series to 177341 cm⁻¹ (739.05 Å, Roig 1976)

no.	$\lambda/\text{Å}$	ν/cm^{-1}	n^*
1	(734.50)	(136147)	(1.63)
2	621.70	160848	2.58
3	592.89	168666	3.56
4	582.79	171587	4.37
5	577.08	173285	5.20
6	573.23	174450	6.16
7	570.95	175147	7.07
8	568.99	175749	8.30
9	567.79	176123	9.49
10	567.36	176255	10.05

This series consists of weak sharp lines and may be due to the excitation of an *ns* electron. The first member of series *a* at 576.11 Å falls between the 5th and 6th series member, and the resulting perturbation is illustrated in figure 5(*g*). Members 8, 9 and 10 are strongly perturbed by the overlapping *e* and *f* series. Although they can be included on an additional branch of the Lu-Fano plot, this is felt to be artificial and they have therefore been omitted from figure 5(*g*). Our calculations of the limit structure are not sufficiently accurate to establish any identification of this series.

TABLE 1 (*cont.*)*(h)* Series to 174555 cm⁻¹ (754.59 Å, Roig 1976)

no.	$\lambda/\text{Å}$	ν/cm^{-1}	n^*
1	(715.69)	(139726)	(1.78)
	(706.43)	(141556)	(1.82)
2	627.91	159260	2.68
	624.11	160228	2.77
3	601.31	166304	3.65
	599.60	166779	3.76
4	590.83	169254	4.59
	589.87	169530	4.67
5	584.95	170956	5.52
	584.27*	171153	5.67
6	581.81	171877	6.40
	581.00	172116	6.70
7	579.37	172600	7.49
	578.94	172728	7.75
8	577.94	173028	8.47
	577.49	173165	8.88
9	577.08	173285	9.29
	576.57	173439	9.91
10		(see note)	
11	575.76	173685	11.23

These are weak sharp series, possibly attributable to the excitation of an *ns* electron. The 10th members are both obscured by the lowest member of series *a* at 576.11 Å which is very broad and intense, and the resulting perturbation is illustrated in figure 5(*h*). Our calculations of the limit structure are not sufficiently accurate to establish any identification of series *h*. The curious behaviour of one of the branches in figure 5(*h*) might indicate that the two series converge on slightly different limits, but the strong perturbation due to the lowest member of channel *a* could equally be responsible.

(i) Series to 169710 cm⁻¹ (near 781.23 Å, Roig 1976)

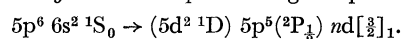
no.	$\lambda/\text{Å}$	ν/cm^{-1}	n^*
1	(753.86)	(132651)	(1.72)
2	648.89	154109	2.65
3	621.70	160848	3.52
4	609.34	164111	4.43
5	602.37	166010	5.45
6	598.53	167075	6.45
7	595.99	167789	7.56
8	594.56	168193	8.50
9	593.54	168482	9.45
10	592.56	168759	10.74
11	591.80	168975	12.22
12	591.34	169108	13.50
—	—	—	—
14	590.83	169254	15.51

This is a weak sharp series, possibly attributable to the excitation of an *ns* electron. The series is perturbed by a number of overlapping channels. There is evidence (figure 5*i*) that 10 and 11 are perturbed by the 592.89 Å transition of channel *g* which lies between them while lower members interact with channel *j* (see figure 5*j*). Our calculations of the limit structure are not sufficiently accurate to establish any identification of this series. The continuum beyond the series limit at 589.24 Å is available for autoionization after photoexcitation by the He resonance line.

TABLE 1 (*cont.*)(j) Series to 169530 cm⁻¹ (784.03 Å, Roig 1976)

no.	$\lambda/\text{Å}$	ν/cm^{-1}	n^*
1	(672.27)	(148750)	(2.30)
2	626.95	159503	3.31
3	611.28	163591	4.30
4	603.63	165664	5.30
5	599.60	166779	6.32
6	597.11	167472	7.30
7	595.43	167945	8.32
8†	594.56	168193	9.06
9†	593.54	168482	10.23

† These transitions are common to channel i and there is evidence of an interaction between channels i and j in the Lu-Fano plot of figure 5(j). Channel j consists of quite strong sharp lines and may be

(k) Series to 166278 cm⁻¹ limit (804.86 Å, Roig 1976)

no.	$\lambda/\text{Å}$	ν/cm^{-1}	n^*
1	(672.27)	(148750)	(2.50)
	(669.15)	(149443)	(2.55)
2	640.46	156137	3.29
	638.38	156646	3.38
3	621.03	161024	4.57
	619.72	161363	4.73
4	614.84	162643	5.49
	613.86	162902	5.70
5	611.28	163591	6.39
	610.41	163824	6.69
6	608.89	164234	7.33
	608.32	164387	7.62
7	607.33	164654	8.32
	606.90	164773	8.54
8	605.99	165018	9.34
	605.57	165133	9.79
9	604.84	165334	10.78
10	604.37	165461	11.59
11	603.99	165564	12.40
12	603.63	165664	13.37
13	603.19	165785	14.92

These excitation channels lie quite low in energy with respect to the others and therefore overlap with a number of possible perturbers. The resulting situation is illustrated by the Lu-Fano plot in figure 5(k). The series are quite strong and sharp and may correspond to

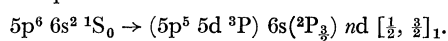


TABLE 1 (*cont.*)*l*) Series to 164705 cm⁻¹ (815.18 Å, Roig 1976)

no.	$\lambda/\text{Å}$	ν/cm^{-1}	n^*
1	(784.31)	(127501)	(1.71)
2	682.12	146603	2.46
3	645.60	154894	3.34
4	630.31	158653	4.26
5	622.94	160529	5.13
6	618.54	161671	6.01
7	615.50	162470	7.01
8	612.36	163302	8.88
9	611.62	163501	9.55
10	610.81	163719	10.55
11	610.41	163824	11.89

This series consists of weak sharp lines and would appear to be an *ns* series converging on the (5p⁵ 5d ³P) 6s ²P_{3/2} limit. The very broad and intense first member of series *e* at 161864 cm⁻¹ overlaps the transitions from no. 5 upwards and strongly perturbs series *l* (see figure 5*l*). Since the series limit at 607.15 Å is to longer wavelengths than 584.3 Å, the continuum in channel *l* is available for auto-ionization after photoexcitation of the He resonance line.

We find that, for each of the series listed in table 1 (*c-l*) it is possible to construct a two-dimensional Lu-Fano plot (see figure 5*c-l*) for which (i) each branch of the curve varies monotonically from left to right and (ii) the entire curve is continuous when translated to opposite edges of the unit square, the rules being obeyed within the limits of experimental error.

We have not attempted to fit theoretical curves $\mu(\nu)$ to the data (Lu & Fano 1970) because these are generally too sparse and because the assumption that two-dimensional plots suffice is very much open to question here. A more appropriate multichannel quantum defect approach would be based on *N*-limit theory rather than the two-limit approach of Lu & Fano (1970). However, the *N*-limit approach is considerably more difficult (see, for example, Armstrong *et al.* 1977) and we have not yet attempted it. For the uppermost series (table 1 *a, b*) we plot quantum defect against energy (figure 5*a, b*).

We find empirically that the data can be sorted self-consistently into channels, i.e. that for each channel a two-dimensional Lu-Fano plot with a limited number of branches can be constructed. The approach is very selective: several ambiguities which would subsist in a simple-minded quantum defect search are resolved. Occasionally, the lowest members lie off the smooth curves, as expected (Lu & Fano 1970). We return to this problem in approach (iii).

TABLE 2. TRENDS OF SOME SLATER-CONDON PARAMETERS FOR 5p-EXCITED CONFIGURATIONS FROM Yb-Ba (ALL VALUES IN cm⁻¹)

parameter	⁷⁰ Yb	⁶⁹ Tm	⁶⁷ Ho	⁶³ Eu	⁵⁹ Pr	⁵⁸ Ce	⁵⁶ Ba I
<i>F</i> ² (5p 5d)	30620	24634	26167	40849	29028	29267	37324
<i>G</i> ¹ (5p 5d)	32924	25190	27180	46872	31166	31646	42612
<i>G</i> ³ (5p 5d)	19752	15033	16273	28665	18839	19224	26290
ζ_{5p}	23454	20707	18483	15841	12590	10066	9401
ζ_{5d}	608	391	397	741	365	323	474

These parameters were obtained from non-relativistic Hartree-Fock calculations for the 5p-excited configurations with either one or the minimum number of 5d electrons. Since the configurations are not isoelectronic, there is no reason for which the parameters should vary smoothly in going from Yb to Ba.

This table is given in support of the trend indicated in figure 3, to show that there is no *dramatic* change in the magnitudes of the Slater-Condon parameters which determine the energy splittings in the 5p subshell spectra.

As Tracy (1977) has pointed out, ζ_{5p} appears to decrease with increasing *Z*, in contrast with the Hartree-Fock calculations. This may indicate that a relativistic treatment is needed for reliable estimates of the parameters.

In general, the Lu-Fano plots are of two kinds. In type 1 a closely similar pattern is obtained if $\nu_{a,b}$ is replaced by energy, which implies that, for such a channel, plotting against $\nu_{a,b}$ is to some extent an arbitrary choice, successful simply because the threshold energy for channels a, b (at $199\,662\text{ cm}^{-1}$) is much higher than the series limit for that channel. Nevertheless, even such an arbitrary Lu-Fano plot is more useful than the plot against energy, because the scale spaces out

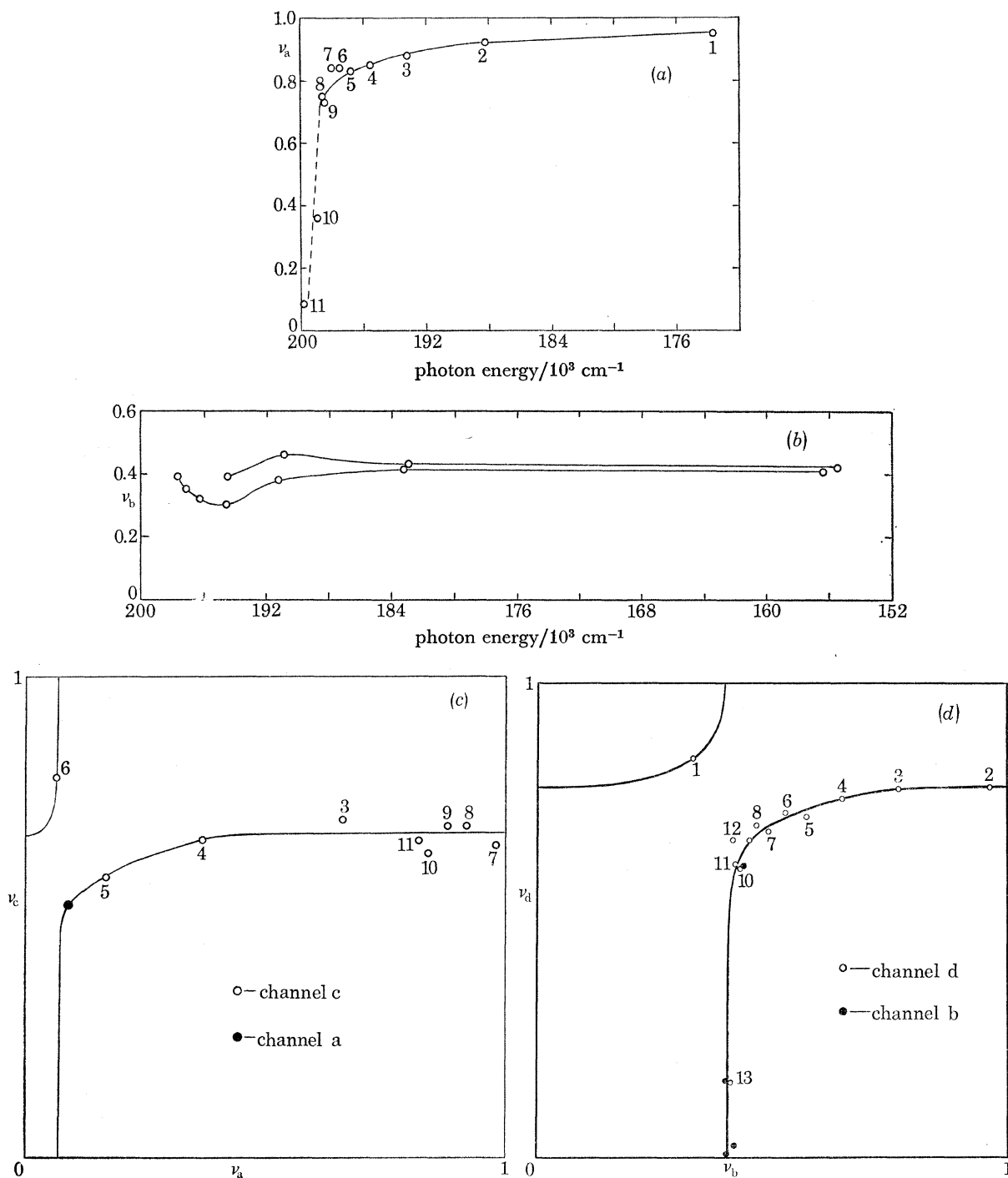


FIGURE 5 (a-d). For description see p. 340.

the experimental points more evenly. In type 2 plots, it is actually possible to find experimental points from another channel which lies on fast changing parts of the curves and can be identified as possible perturbers. Type 2 plots contain potentially more information than a simple plot against energy and may imply some coupling between the channels.

From the practical point of view of sorting the lines into channels, plots against $\nu_{a,b}$ proved most useful and were found to work in all cases. The method does not, however, yield any information about the nature of the channels concerned, since the thresholds remain unidentified. The plots must therefore be supplemented by an analysis of the limit system. Unfortunately, (see

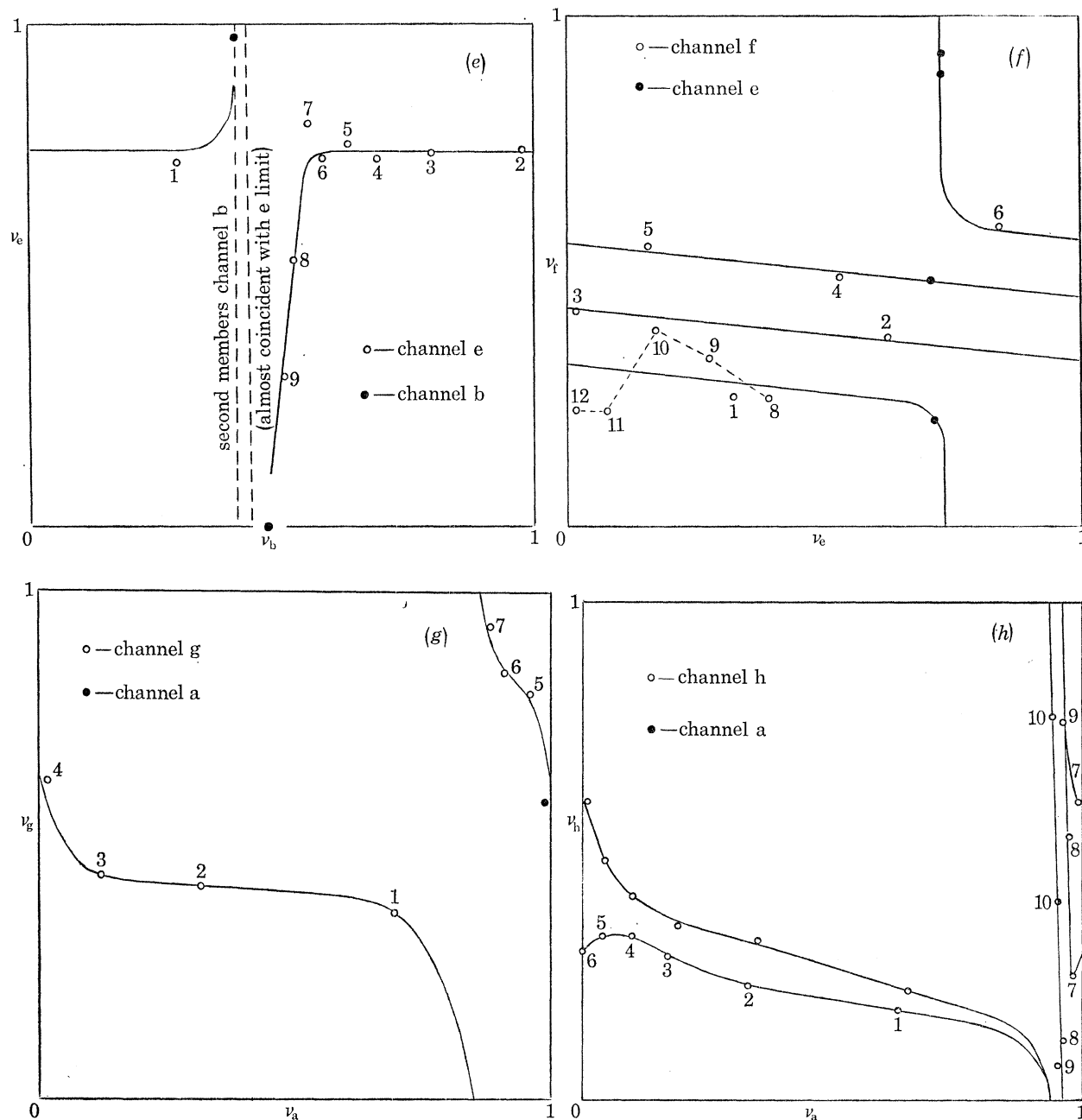


FIGURE 5 (e-h). For description see p. 340.

below) the $5p$ spectrum of Ba II is not yet well understood. Approaches (ii) and (iii) have been used in an attempt to resolve this difficulty.

Finally, one might expect that two-dimensional Lu-Fano plots would be much more appropriate to the closely related problem of the intense series in Yb I (Tracy 1977) attributed to the transitions

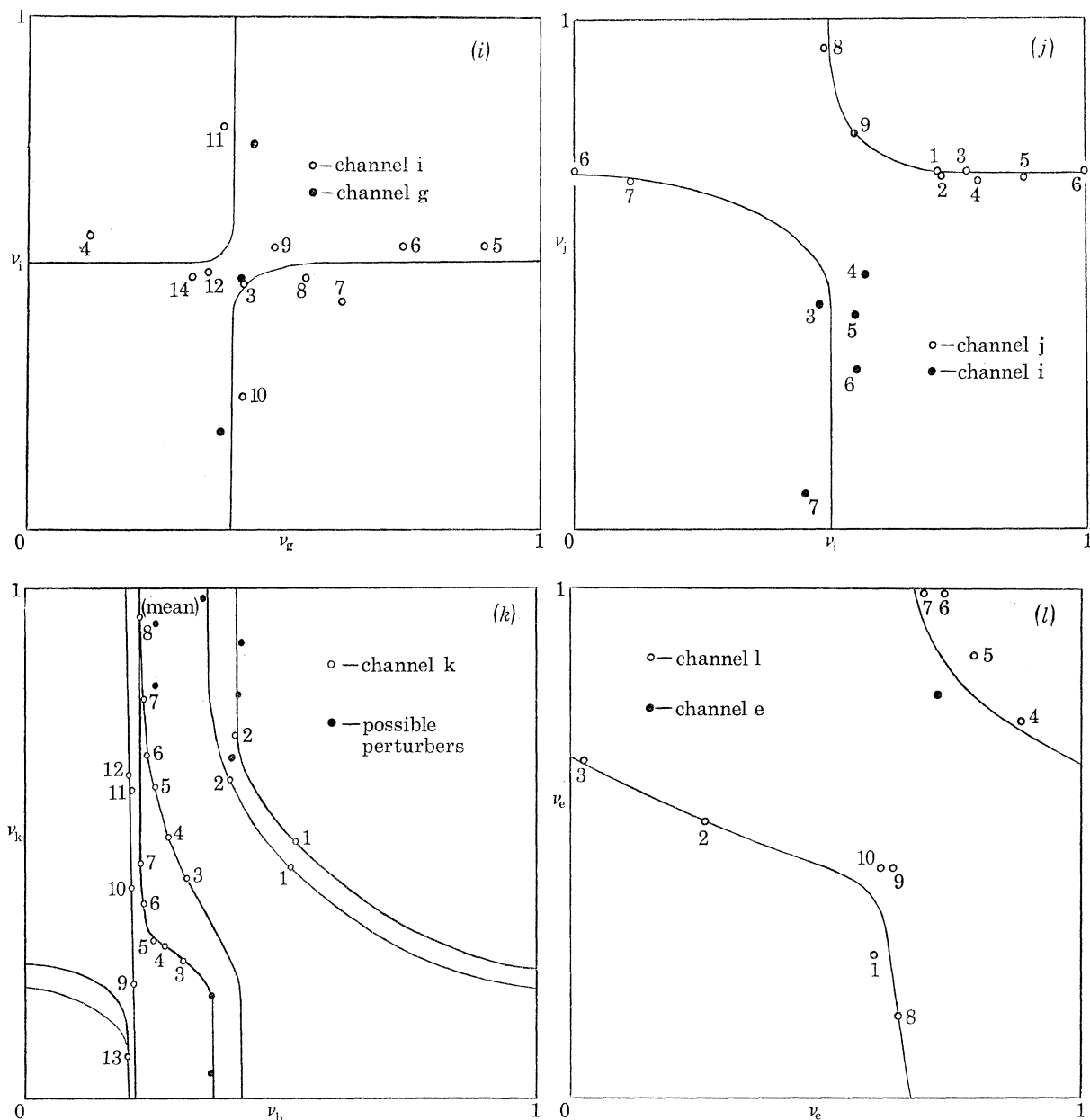
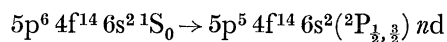


FIGURE 5. (a) Quantum defect plot for channel a. (b) Quantum defect plot for channel b. (c) Lu-Fano plot for channels c, a. (d) Lu-Fano plot for channels d, b. (e) Lu-Fano plot for channels e, b. (f) Lu-Fano plot for channels f, e. (g) Lu-Fano plot for channels g, a. (h) Lu-Fano plot for channels h, a. (i) Lu-Fano plot for channels i, g. (j) Lu-Fano plot for channels j, i. (k) Lu-Fano plot for channels k, b. (l) Lu-Fano plot for channels l, e.

(cf. approach (ii) below) which give some idea of what the appearance of the Ba I 5p spectrum might be in absence of strong s-d mixing. Unfortunately, the data are few and their distribution such that no reliable conclusion can be reached.

The series labelled *a* and *b* are among the most intense in the Ba spectrum and give rise to the most prominent limit (at $199\,662\text{ cm}^{-1}$), partly because they converge in an energy range where the Ba spectrum simplifies (cf. Connerade 1970*a*).

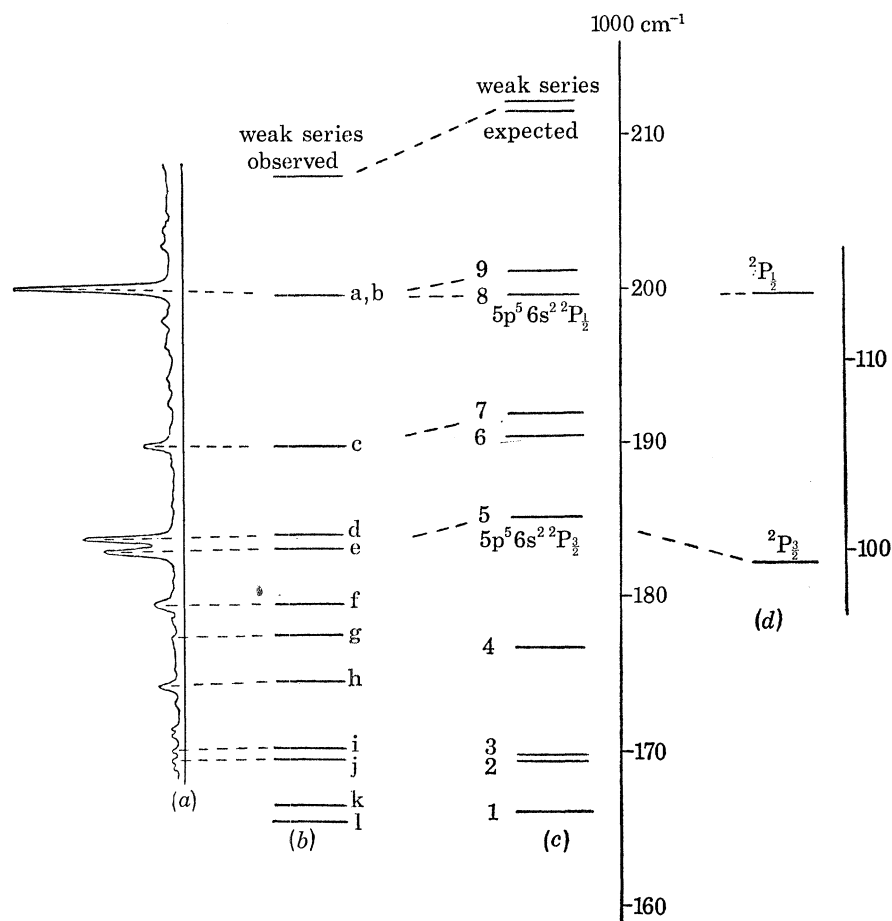


FIGURE 6. (a) 5p binding energies in Ba II as measured by Mehlhorn *et al.* (1977). (b) 5p limit structure in Ba I as deduced from the present empirical series classification. Note the excellent agreement with Mehlhorn *et al.* (1978). (c) 5p limit structure in Ba I as deduced from Hartree-Fock calculations (table 3*f*). In order to emphasize the difficulties of interpretation, only those levels with more than 10% 3P character have been included. If *all* the levels are included, it is possible to account for the number of observed series, but not for their intensities, and the accuracy of the calculations is not sufficient for detailed identifications to be made (see text). (d) Present interpretation of $5p^5 6s^2$ in Cs I (see table 4).

Since the present analysis was performed, measurements of the 5p binding energy have been communicated to us by Mehlhorn *et al.* (1977). The very good correspondence between these measurements and our analysis of the Ba I series is shown in figure 6 and illustrates how complementary information can be obtained from electron impact and photoabsorption experiments.

Approach (ii)

Approach (ii) stems from the work of Tracy (1977) on 5p excitation of the lanthanides, where it was found (Tracy 1977, fig. 2) that the gross structure of the absorption spectra can be followed

back from Yb to Sm. Connerade & Tracy (1977) have suggested (i) that the most prominent absorption feature for the elements Yb–Sm is the giant (5p; 5d) 1P resonance predicted by Wendin (1973, 1974), and (ii) that the apparent absence of this feature from the spectrum of Ba I and La I could be attributed to s–d mixing (Connerade 1970*a, b*). It is therefore to be expected that the $5p^5 5d ^1P_1$ characterization in Ba I will, in fact, be ‘split up’ among many upper levels.

The energy dependence of several transitions on atomic number has been followed from Yb to Dy and, for the ‘giant resonance’, from Yb to Sm (Tracy 1977). It is nearly linear and, extrapolating out as far as Ba I would place the ‘giant resonance’ at $172\,232\text{ cm}^{-1}$ (581 Å).

Tracy (1977) has also shown that Hartree–Fock atomic structure calculations do not yield the correct Z -dependence of the spin-orbit parameter ζ_{5p} . This empirical extrapolation is therefore preferable to any non-relativistic attempt at calculating the energy of the $5p^5 5d ^1P_1$ level. Since the upper level of the (5p; 5d) 1P_1 ‘giant resonance’ is also the initial excited state in Hansen’s (1975) two-step autoionization process, the high rate of double ionization observed when Ba I is excited by 584.3 Å radiation is consistent with our extrapolation. An absorption line occurs at 584.27 Å (see table 1*h*) which clearly must possess some $5p^5 6s^2 5d ^1P_1$ character, but this presumably arises through mixing because this line is not particularly intense and does not belong to an especially intense series.

What appears more significant is that the first member of series *a* (at 576.11 Å, table 1*a*) and the second member of series *e* (at 579.37 Å, table 1*e*) both of which are extremely broad, occur in a region of high absorption (see figure 2), fairly close to 580 Å.

A plausible interpretation is that series *a* consists of

$$5p^6 6s^2 ^1S_0 \rightarrow 5p^5 6s^2 (^2P_{\frac{3}{2}}) ns, nd$$

transitions, converging on the $5p^5 6s^2 ^2P_{\frac{3}{2}}$ limit, in which case the level at $173\,578\text{ cm}^{-1}$ (576.11 Å transition) would contain most $5p^5 6s^2 5d ^1P_1$ character. Series *e* would be

$$5p^5 6s^2 ^1S_0 \rightarrow 5p^5 6s^2 (^2P_{\frac{3}{2}}) nd,$$

the first member of which is also very broad and intense and the second of which (at 579.37 Å) lies near $5p^5 6s^2 5d ^1P_1$.

Approach (iii)

In this approach, we have performed unrestricted Hartree–Fock calculations for 5p-excited configurations in Cs I, Ba I and several of the elements La–Yb, results of which are summarized in table 3 (*a–e*).

An important point is that the Connerade’s (1970*a*) type 1 double excitation (see above) can only be applied satisfactorily to members higher than the first in the $5p^6$ – $5p^5(5d \times 6s)$ *ns, nd* series. For the first series members (e.g. $5p^5 6s^2$, $5p^5 5d 6s$, $5p^5 5d^2$, etc.) interactions between the running electron and the extended core are comparable in magnitude with interactions within the core. The distribution of levels in the lowest 5p-excited configurations therefore does not follow that of the limits (i.e. they depart strongly from $J_c K$ coupling) and transitions to $5p^5 5d 6s$, $5p^5 5d^2$, etc., occur through mixing after coupling the excited electron (type 2 double excitation). It is therefore appropriate to consider separately calculations of the Ba I $5p^5(6s \times 5d)$ limit structure and calculations of the lowest 5p-excited configurations and then examine their relation to the Lu–Fano plots considered in (i) above.

5p ABSORPTION SPECTRA OF Ba I, Cs I

343

TABLE 3

(a) Hartree-Fock parameters for 5p-excited configuration in Ba II (all values in cm^{-1} referred to the Ba I ground state)

	5p ⁵ 5d 6s	5p ⁵ 5d ²	5p ⁵ 6p ²
E_{av}	140392	138463	191632
F^2 (5p 5d)	39028	36332	—
G^1 (5p 5d)	44915	41267	—
G^3 (5p 5d)	27794	25409	—
G^1 (5p 5s)	3574	—	—
G^2 (5d 6s)	12988	—	—
F^2 (6p 6p)	—	—	21872
F^2 (5p 6p)	—	—	11329
G^0 (5p 6p)	—	—	1810
G^2 (5p 6p)	—	—	2541
F^2 (5d 5d)	—	33963	—
F^4 (5d 5d)	—	22233	—
ζ_{5p}	9439	9190	9900
ζ_{5d}	512	443	—
ζ_{6p}	—	—	959

(b) Hartree-Fock parameters for 5p-excited configurations in Ba I (all values in cm^{-1} referred to the Ba I ground state; radii in atomic units)

parameters	5p ⁵ 5d ³	5p ⁵ 5d ² 6s	5p ⁵ 5d 6s ² (average)	5p ⁵ 5d 6s ² (¹ P)	5p ⁵ 6s ² 6d
E_{av}	148055	140903	138634	165149	174946
F^2 (5p nd)	30102	33997	37324	13336	2177
G^1	32992	38138	42612	9531	1621
G^3	20130	23400	26290	5810	1042
F^2 (nd nd)	27485	31389	—	—	—
F^4	17583	20360	—	—	—
G^1 (5p 6s)	—	2410	—	—	—
G^2 (nd 6s)	—	11813	—	—	—
ζ_{5p}	9041	9182	9401	9772	9724
ζ_{nd}	326	399	474	56	22
$\langle r_{5p} \rangle$	1.948	1.9350	1.9163	1.8840	1.8893
$\langle r_{nd} \rangle$	3.590	3.2189	2.9616	5.4275*	12.2950
$\langle r_{6s} \rangle$	—	5.4086	5.0583	4.6829	4.3879

* Note the large effect of wavefunction expansion on the 5p⁵ 5d 6s²(¹P) state, illustrated in figure 8.(c) Intermediate coupling calculation of the 5p⁵ 5d 6s² configuration of Ba I

designation	calculated energy	composition (<i>LS</i> basis)
³ P ₀	121790	100 ³ P ₀
¹ P ₁	165149*	14 ³ D ₁ ⟩ + 6 ³ P ₁ ⟩ + 99 ¹ P ₁ ⟩
³ D ₁	143915	97 ³ D ₁ ⟩ + 19 ³ P ₁ ⟩ - 15 ¹ P ₁ ⟩
³ P ₁	123549	-19 ³ D ₁ ⟩ + 98 ³ P ₁ ⟩ - 3 ¹ P ₁ ⟩
³ D ₂	147700	4 ³ F ₂ ⟩ + 74 ³ D ₂ ⟩ - 57 ¹ D ₂ ⟩ + 37 ³ P ₂ ⟩
¹ D ₂	144962	65 ³ F ₂ ⟩ + 44 ³ D ₂ ⟩ + 62 ¹ D ₂ ⟩
³ F ₂	133228	76 ³ F ₂ ⟩ - 41 ³ D ₂ ⟩ - 50 ¹ D ₂ ⟩ - 6 ³ P ₂ ⟩
³ P ₂	127033	3 ³ F ₂ ⟩ - 32 ³ D ₂ ⟩ + 20 ¹ D ₂ ⟩ + 93 ³ P ₂ ⟩
¹ F ₃	149061	-45 ³ F ₃ ⟩ + 69 ¹ F ₃ ⟩ - 57 ³ D ₃ ⟩
³ D ₃	137887	-3 ³ F ₃ ⟩ + 62 ¹ F ₃ ⟩ + 78 ³ D ₃ ⟩
³ F ₃	130144	89 ³ F ₃ ⟩ + 36 ¹ F ₃ ⟩ - 26 ³ D ₃ ⟩
³ F ₄	128307	100 ³ F ₄ ⟩

* The energy given here corresponds to a separate variational calculation for this level. Configuration average parameters yield an energy of 184937 cm^{-1} . The composition is given within the configuration average approximation. The value of n^* appropriate for this configuration ranges from 1.53 (average) to 2.34 (for ¹P₁).

TABLE 3 (cont.)

(d) Intermediate coupling calculations for the $5p^5 6s^2 6d$ configuration of Ba I

designa- tion	calculated energy	composition (<i>LS</i> basis)	composition (<i>jj</i> basis)
$(\frac{3}{2}, \frac{3}{2})_0$	169 463	$100 ^3P_0\rangle$	$100 \frac{3}{2}, \frac{3}{2}, 0 \rangle$
$(\frac{1}{2}, \frac{3}{2})_1$	185 246	$69 ^3D_1\rangle + 38 ^3P_1\rangle + 61 ^1P_1\rangle$	$5 \frac{3}{2}, \frac{5}{2}, 1 \rangle + 100 \frac{1}{2}, \frac{3}{2}, 1 \rangle$
$(\frac{3}{2}, \frac{5}{2})_1$	171 166	$-60 ^3D_1\rangle - 18 ^3P_1\rangle + 78 ^1P_1\rangle$	$89 \frac{3}{2}, \frac{5}{2}, 1 \rangle - 45 \frac{3}{2}, \frac{3}{2}, 1 \rangle - 5 \frac{1}{2}, \frac{3}{2}, 1 \rangle$
$(\frac{3}{2}, \frac{3}{2})_1$	169 649	$-40 ^3D_1\rangle + 91 ^3P_1\rangle - 10 ^1P_1\rangle$	$45 \frac{3}{2}, \frac{5}{2}, 1 \rangle + 89 \frac{3}{2}, \frac{3}{2}, 1 \rangle - 3 \frac{1}{2}, \frac{3}{2}, 1 \rangle$
$(\frac{1}{2}, \frac{5}{2})_2$	184 551	$-15 ^3F_2\rangle - 61 ^3D_2\rangle + 39 ^1D_2\rangle - 68 ^3P_2\rangle$	$3 \frac{3}{2}, \frac{5}{2}, 2 \rangle + 1 \frac{3}{2}, \frac{3}{2}, 2 \rangle + 100 \frac{1}{2}, \frac{5}{2}, 2 \rangle + 3 \frac{1}{2}, \frac{3}{2}, 2 \rangle$
$(\frac{1}{2}, \frac{3}{2})_2$	184 488	$86 ^3F_2\rangle + 21 ^3D_2\rangle + 45 ^1D_2\rangle - 12 ^3P_2\rangle$	$1 \frac{3}{2}, \frac{5}{2}, 2 \rangle - 1 \frac{3}{2}, \frac{3}{2}, 2 \rangle - 3 \frac{1}{2}, \frac{5}{2}, 2 \rangle + 100 \frac{1}{2}, \frac{3}{2}, 2 \rangle$
$(\frac{3}{2}, \frac{3}{2})_2$	170 215	$-48 ^3F_2\rangle + 51 ^3D_2\rangle + 71 ^1D_2\rangle + 5 ^3P_2\rangle$	$-46 \frac{3}{2}, \frac{5}{2}, 2 \rangle + 89 \frac{3}{2}, \frac{3}{2}, 2 \rangle + 2 \frac{1}{2}, \frac{3}{2}, 2 \rangle$
$(\frac{3}{2}, \frac{5}{2})_2$	169 930	$3 ^3F_2\rangle - 57 ^3D_2\rangle + 38 ^1D_2\rangle + 73 ^3P_2\rangle$	$89 \frac{3}{2}, \frac{5}{2}, 2 \rangle + 46 \frac{3}{2}, \frac{3}{2}, 2 \rangle - 3 \frac{1}{2}, \frac{5}{2}, 2 \rangle$
$(\frac{1}{2}, \frac{5}{2})_3$	184 670	$66 ^3F_3\rangle - 58 ^1F_3\rangle + 48 ^3D_3\rangle$	$100 \frac{1}{2}, \frac{5}{2}, 3 \rangle - 1 \frac{3}{2}, \frac{3}{2}, 3 \rangle$
$(\frac{3}{2}, \frac{5}{2})_3$	170 328	$-14 ^3F_3\rangle + 53 ^1F_3\rangle + 84 ^3D_3\rangle$	$100 \frac{3}{2}, \frac{5}{2}, 3 \rangle - 1 \frac{1}{2}, \frac{3}{2}, 3 \rangle$
$(\frac{3}{2}, \frac{3}{2})_3$	169 961	$74 ^3F_3\rangle + 62 ^1F_3\rangle - 26 ^3D_3\rangle$	$1 \frac{3}{2}, \frac{5}{2}, 3 \rangle + 1 \frac{1}{2}, \frac{5}{2}, 3 \rangle + 100 \frac{3}{2}, \frac{3}{2}, 3 \rangle$
$(\frac{3}{2}, \frac{5}{2})_4$	169 829	$100 ^3F_4\rangle$	$100 \frac{3}{2}, \frac{5}{2}, 4 \rangle$

The calculations show clearly that the *jj* coupling scheme is much more appropriate for this configuration than the *LS* scheme. Nevertheless, compositions in *LS* coupling are given for comparison with table 3 (c). The value of n^* appropriate for this configuration is estimated as 3.26.

(e) Hartree-Fock parameters for $5p^5 4f^2$ (all values in cm^{-1} referred to the Ba I ground state)

E_{av}	= 256 955	$G^2(5p 4f)$	= 25 544
$F^2(4f 4f)$	= 31 592	$G^4(5p 4f)$	= 17 743
$F^4(4f 4f)$	= 18 708	ζ_{5p}	= 8 471
$F^6(4f 4f)$	= 13 189	ζ_{4f}	= 194
$F^2(5p 4f)$	= 34 875	$\langle r_{5p} \rangle$	= 1.9876
$F^4(5p 4f)$	= 20 550	$\langle r_{4f} \rangle$	= 2.8218

(f) Calculated energies of $5p$ -excited $J = \frac{1}{2}$ and $J = \frac{3}{2}$ levels with more than 10% 2P character in Ba^+

no.	configuration	designation	2P content (%)	energy
1	$(5p^5 5d) 6s$	$(^3P) ^2P_{\frac{1}{2}}$	93	127 845
2	$5d^2 5p^5$	$(^1D) ^2P_{\frac{1}{2}}$	18	131 233
3	$(5p^5 5d) 6s$	$(^3P) ^2P_{\frac{3}{2}}$	82	131 453
4	$5d^2 5p^5$	$(^1D) ^2D_{\frac{3}{2}}$	14	138 654
5	$6s^2 5p^5$	$(^1S) ^2P_{\frac{3}{2}}$	100	147 047
6	$(5p^5 5d) 6s$	$(^3D) ^2D_{\frac{3}{2}}$	11	152 363
7	$5d^2 5p^5$	$(^1S) ^2P_{\frac{3}{2}}$	66	153 806
8	$6s^2 5p^5$	$(^1S) ^2P_{\frac{1}{2}}$	100	161 651
9	$5d^2 5p^5$	$(^1S) ^2P_{\frac{1}{2}}$	74	163 081
10	$(5p^5 5d) 6s$	$(^1P) ^2P_{\frac{1}{2}}$	95	173 613
11	$(5p^5 5d) 6s$	$(^1P) ^2P_{\frac{3}{2}}$	95	174 135
12	$5d^2 5p^5$	$(^3P) ^2P_{\frac{3}{2}}$	21	180 966
13	$6p^2 5p^5$	$(^1S) ^2P_{\frac{3}{2}}$	76	197 359
14	$6p^2 5p^5$	$(^1S) ^2P_{\frac{1}{2}}$	98	212 400

The calculations are performed in full intermediate coupling with separate variational treatment of certain high terms but no allowance for shifts due to configuration mixing. Energies are given in cm^{-1} above the Ba^+ ground state.

It is, of course, the $5p^5 6s^2$ 2P content values rather than the 2P content of the levels which determines their prominence as series limits in Ba^+ . However, our calculations do not include mixing between configurations, and the 2P content is therefore the only guide available to us.

Calculations of the $5p^5 5d 6s$ level structure were reported by Hansen (1974) who identified four thresholds reported by Peart *et al.* (1973) in electron impact ionization of Ba^+ at 15.8, 16.8, 19.2 and 21.9 eV. The calculations were performed in intermediate coupling using empirically scaled non-relativistic Hartree–Fock parameters. Hansen (1974) regarded the identification of three of the thresholds as $(5p^5 5d^3 P) 6s^2 P_{\frac{1}{2}}$, $(5p^5 5d^3 P) 6s^2 P_{\frac{3}{2}}$ and $(5p^5 5d^1 P) 6s^2 P_{\frac{1}{2}, \frac{3}{2}}$ as fairly certain, with the identification of the fourth (at 19.2 eV) being somewhat more tentative.

After some further experiments by Peart & Dolder (1975) on electron impact excitation cross-sections for the corresponding configurations in Ca^+ and Sr^+ , Hansen (1975) returned to the problem with some consideration of the excitation mechanism and the inclusion of configuration mixing. The situation then appeared less clear and it emerged that final verification of Hansen's (1974) identifications would require elaborate calculations of the coulomb exchange contribution to the excitation cross-section.

In the later paper, Hansen (1975) includes mixing between four configurations of Ba II, namely $5p^5 5d 6s$, $5p^5 6s^2$, $5p^5 5d^2$ and $5p^5 6p^2$. He finds that $5p^5 5d(1P) 6s^2 P$ and $5p^5 5d(3P) 6s^2 P$ are 72 % and 77 % pure respectively with admixtures of up to 15 % from $5p^5 5d^2$. Because of the near-energy degeneracy between terms of $5p^5 5d 6s$ and $5p^5 5d^2$, mixing between these two configurations is much more severe than mixing between $5p^5 5d 6s$ and $5p^5 6p^2$. Nevertheless, Hansen (1975) concludes that the energy displacements caused by the $(5p^5 5d 6s) - 5p^5(5d^2 \times 6s^2)$ interaction are at most 1600 cm^{-1} , and that the identifications of Hansen (1974) should still be retained since they agree well with the experimental energies and with the number of observed thresholds. It should be noted that the experimental accuracy claimed by Peart *et al.* (1973) is of about $\pm 1200 \text{ cm}^{-1}$.

The absorption spectrum of Ba^+ was studied by Roig (1976), who comments that the auto-ionization thresholds of Peart *et al.* (1973) appear to correspond to very broad resonances but that, because transitions from both the ground and metastable states are superposed in the absorption spectrum, the resonances are almost completely blended. Roig (1976) observed five series converging on the three limits $5p^5(2P_{\frac{3}{2}}) 6s[\frac{3}{2}]_2$, $5p^5(2P_{\frac{3}{2}}) 6s[\frac{3}{2}]_1$ and $5p^5(2P_{\frac{1}{2}}) 6s[\frac{1}{2}]_1$ identified by Reader & Epstein (1975). If these are $5p \rightarrow nd$ series, then the resonances corresponding to the Peart *et al.* (1973) thresholds would be the first members. However, relating the Peart *et al.* (1973) energy measurements to Reader & Epstein's (1975) $5p^5 6s$ energy measurements yields effective quantum numbers $n^* \approx 1.0\text{--}1.2$. It is well known (Griffin *et al.* 1969) that collapse of the $5d$ wavefunction around atomic numbers $Z = 57$ can lead to values of $n^* \approx 1.4$. When a $5p$ vacancy is created, Ba I might well be expected to resemble valence-excited La I but values of $n^* \approx 1.0\text{--}1.2$ nevertheless seem too low for $5p \rightarrow 5d$ excitation. Our own Hartree–Fock estimates of n^* are as follows: 1.53(5d), 2.34(5d 1P), 3.26(6d), 2.71(7s).

By approach (i) we have extracted 12 series limits, the distribution of which is shown in figure 6.

From previous work on Cs, Ba and related spectra cited above, it is clear that all the configurations $5p^5 6s^2$, $5p^5 5d 6s$ and $5p^5 5d^2$ must be considered as possible limit systems for the photo-absorption spectrum. Also, from Hansen's (1975) work, it follows that energy shifts due to configuration mixing do not appear to exceed 1200 cm^{-1} . It therefore seems reasonable, in a first approximation, to compute the energies of all the $J = \frac{1}{2}$ and $\frac{3}{2}$ levels in the three relevant configurations without the inclusion of mixing, taking care, however, to apply Hansen's (1974) procedure of separate variational calculations for levels based on the high lying $5p^5 5d^1 P$ parent.

The Hartree–Fock calculations yield average energies and Slater–Condon parameters listed in tables 3(a–e); in table 3(f) we list the levels with more than 10 % 2P character from the con-

figurations which appear most likely ($5p^5 4f^2$ occurs too high in energy to be of significance here). The energy spanned by these levels is $85\,000\text{ cm}^{-1}$ as against a span of $34\,000\text{ cm}^{-1}$ in the observed series limits. If the two $6p^2 5p^5(^1S) ^2P$ levels are excluded, then the calculated span is reduced to $53\,121\text{ cm}^{-1}$ and there are enough levels with significant 2P character to account for the number of observed series.

Unfortunately, as mentioned above, these single configuration non-relativistic Hartree–Fock plus intermediate coupling calculations are not sufficiently accurate to yield energy intervals reliably.

If we compare with similar spectra, the supernumerary $3p$ limit in Ca I, additional to

$$3p^5 4s^2 ^2P_{\frac{1}{2}, \frac{3}{2}}$$

(Mansfield & Newsom 1977), has been reliably identified as $3p^5(3d^2 ^1S) ^2P_{\frac{3}{2}}$. Both the

$$3p^5(3d^2 ^1S) ^2P_{\frac{1}{2}} \quad \text{and} \quad ^2P_{\frac{3}{2}}$$

resonances can be seen in the electron impact data for Ca (Schmitz *et al.* 1976; Pejčev *et al.* 1978). The experimental evidence puts the $3p^5 4s^2 \times 3p^5 3d^2$ mixing at 10% in Ca^+ , and the calculated s^2 – d^2 energy gap is smaller for Ba^+ than for Ca^+ , so that the mixing would be expected to rise sharply. On the other hand ($3p^5 3d ^3P$) $4s ^2P_{\frac{1}{2}}$ and $^2P_{\frac{3}{2}}$ limits were not detected in Ca I (Mansfield & Newsom 1977) although they lie in an energy region where the structure is relatively open. The relative energy shifts between configurations required to bring the calculations into approximate correspondence with experiment for Ca^+ were of the order of $11\,000\text{ cm}^{-1}$ maximum, which is an indication of the accuracy to be expected for Ba^+ .

In figure 6, we show a comparison between the results of our calculations and the observed distribution of limits, as deduced from the Lu–Fano plots. From this comparison, it is clear that improved calculations would be required to make a specific assignment for each limit. Nevertheless, the calculations confirm that the relevant configurations are $5p^5 6s^2$, $5p^5 5d^2$ and $5p^5 5d 6s$. A fully relativistic multiconfiguration Dirac–Fock treatment (e.g. Rose *et al.* 1978) would seem necessary. Within our simplified approach we have been able to draw three conclusions (*a*, *b*, *c* below) which may be useful for further work.

(a) *The importance of 5d wavefunction expansion.* In any attempt to describe the

$$5p^5(6s^2 \times 6s 5d \times 5d^2)$$

configuration mixing by radial integrals, an average of configuration approach may prove inadequate: a significant expansion of $5d$ orbitals can occur among the high levels of $5p$ -excited configurations, and this would clearly affect the configuration mixing matrix elements differently for different levels (figure 7).

(b) *The identification of the $5p^5 6s^2 ^2P_{\frac{1}{2}, \frac{3}{2}}$ thresholds.* Within a one-electron excitation scheme, the $5p^5 6s^2 ^2P_{\frac{1}{2}}$ and $^2P_{\frac{3}{2}}$ thresholds are the only allowed series limits. According to our calculations, they lie relatively low (5 and 8 in table 3(*f*)) compared with other series limits. The tentative identification of the *a*, *b* threshold as mainly $5p^5 6s^2 ^2P_{\frac{1}{2}}$ reached in part (ii) is nevertheless consistent with the comparison (figure 6) between calculated and observed limit distributions, particularly when the interpretation of the very weak series (*c*, below) is considered.

If this interpretation is accepted, the calculations also suggest that the $5p^5 6s^2 ^2P_{\frac{3}{2}}$ limit must lie somewhere in the vicinity of the limits labelled *d* and *e* (see figure 6), in which case the rather intense series (*e*) is probably an *nd* series converging on $5p^5 6s^2 ^2P_{\frac{3}{2}}$ as suggested above.

Multiconfiguration Dirac–Fock s.c.f. calculations by Rose *et al.* (1978) show that the ground

state of Ba I is 92 % pure $5p^6 6s^2 1S_0$ and contains (6 % $6p^2 1S_0$ + 1 % $5d^2 1S_0$). We therefore expect a weak i.s.c.i. spectrum, $6s^2$ characterization being essentially 'pure' in the ground state. The experimental evidence from the 3p spectrum of Ca I (Mansfield & Newsom 1977) also supports this view.

The occurrence of many supernumerary series in the 5p spectrum of Ba I shows that the $6s^2$ subshell is shattered by 5p excitation, i.e. that the spectator electron approximation (cf. Connerade *et al.* 1977) breaks down completely for the 6s subshell, with f.i.s.c.i. as the dominant excitation mechanism for the supernumerary series.

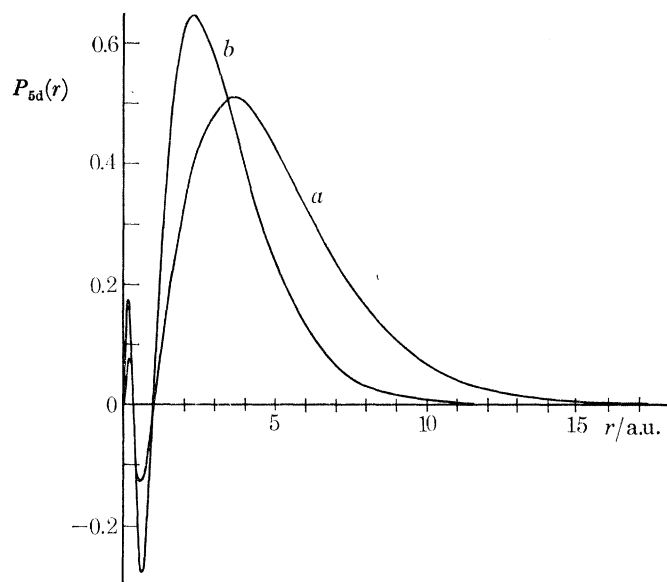


FIGURE 7. Expansion of the 5d wavefunction in Ba II ($5p^5 5d 1P$) 6s (*a*), compared with $5p^5 5d 6s$ configuration average (*b*).

(*c*) *The interpretation of very weak series above 200 000 cm⁻¹.* Some very weak series converge to limits higher than *a*, *b* (see figure 6) but are too weak for accurate measurement. In Cs I (Connerade 1970*a*) similar weak series were found, and attributed to double excitations of type 2 (see above) converging on $5p^5 6p$ limits. However, Roig (1976) following Reader & Epstein (1975) suggests that the weak series in Cs I might in fact converge on $5p^5 5d 1P_1$, in which case the whole of the 5p-excitation spectrum in Cs I would be dominated by type 1 double excitations (Connerade 1970*a*).

Roig's (1976) suggestion is attractive because one could explain the weakness of the high series as a consequence of 5d wavefunction expansion in $5p^5 5d 1P_1$ (see (*a*) above) which would reduce configuration mixing between $5p^5 6s$ and $5p^5 5d 1P_1$. However, comparisons with related spectra suggest that the situation is not quite so simple.

In K I (Mansfield 1975) a clear series can be followed to $3p^5 3d 1P_1$, confirming that the expansion of the 3d wavefunction reduces but does not eliminate configuration mixing for the high $1P_1$ term. However, type 2 double excitations (Connerade 1970*a*) to even parity limits ($3p^5 4p 1S_0$ and $3S_1$ in K I and $2p^5 3p 1S_0$ and $3S_1$ in Na I, Mansfield unpublished) also occur quite clearly. Probably, the structure in Cs I is a mixture of type 1 and type 2 transitions to $5p^5 5d 1P_1$ and $5p^5 6p$ limits respectively. In Ba II (Roig 1976) the $5p^5 6p$ limits are presumably higher and can be excluded.

Returning to Ba I, one would expect $5p^5 5d(1P) 6s^2 P_{\frac{1}{2}}$ and $2P_{\frac{3}{2}}$ to be diminished in importance by $5d$ wavefunction expansion, so that only weak series to limits 10 and 11 would be seen. This conclusion is consistent with our comparison in figure 6. From the calculations, $5p^5 6p^2$ is high and can be excluded, while $5d^2(3P) 5p^5 2P_{\frac{1}{2}}$ (limit 12) is not subject to significant $5d$ wavefunction expansion (see table 3).

We turn now to the lowest energy configurations and begin by considering Cs I because it is isoelectronic with Ba II. Approach (iii) is the most relevant here because the concept of type 1 double excitations (Connerade 1970*a*) defined by reference to the parent ion spectrum is mainly applicable to upper series members (Mansfield & Newsom 1977). A first point which appears to have been overlooked so far is that, if Beutler & Guggenheimer's (1934) assignment for the transitions to $5p^5 6s^2 2P_{\frac{1}{2}}$ and $2P_{\frac{3}{2}}$ is adopted, the splitting of 9813 cm^{-1} is greatly at variance both with calculated values and with other observational derivations of ζ_{5p} in this region of the periodic table. A splitting approaching 13000 cm^{-1} would be expected, though it is difficult to find transitions with this interval.

TABLE 4. NEW IDENTIFICATIONS FOR LOW ENERGY TRANSITIONS IN THE $5p$ SPECTRUM OF Cs I

energy/cm ⁻¹	identification
99256	$5p^5 6s^2 2P_{\frac{3}{2}}$
113488	$5p^5 6s^2 2P_{\frac{1}{2}}$
103119*	$5p^5 5d 6s 4P_{\frac{1}{2}}$
104280*	$5p^5 5d 6s 4P_{\frac{3}{2}}$
106490*	$5p^5 5d 6s 4P_{\frac{5}{2}}$
106383†	$5p^5 5d(3P) 6s 2P_{\frac{1}{2}}$
109150	$5p^5 5d(3P) 6s 2P_{\frac{3}{2}}$

An extensive revision of the analysis of the Cs I spectrum is in progress. The original analysis (Connerade 1970*a*) will be substantially improved because of the revision of the Cs II analysis mentioned in the Introduction and because lower series members do not conform to $J_c K$ coupling (Mansfield & Newsom 1977).

* From Pejčev & Ross (1977).

† New observation.

We have performed intermediate coupling diagonalizations of $5p^5 6s^2$, $5p^5 5d 6s$, $5p^5 5d^2$ and $5p^5 6s 7s$ using Slater–Condon parameters obtained from Hartree–Fock calculations. The agreement between theory and experiment is worse than for the corresponding cases in K I (Mansfield 1975) or Rb I (Mansfield 1978). The calculations suggest that the $2P_{\frac{3}{2}}$ assignment of Beutler & Guggenheimer (1934) is correct but that $2P_{\frac{1}{2}}$ corresponds to the transition at 881 \AA . As a result of these calculations and of further comparisons with electron energy loss spectra of Cs I obtained by Pejčev & Ross (1977) in which the $5p^5 5d 6s 4P_{\frac{1}{2}, \frac{3}{2}, \frac{5}{2}}$ levels can be picked out, several $5p^5 5d 6s$ levels have also been identified. A list of new assignments for Cs I is given in table 4 and a comparison with Ba II is shown in figure 6.

A general point about the analysis of the $5p$ spectrum of Cs I is that $5p^5 5d 6s$ and $5p^5 5d^2$ occur lower in relation to the $5p^5 6s^2$ energy than do corresponding configurations in the other alkalis. Thus, for Cs I, $5p^5 5d 6s$ overlaps $5p^5 6s^2$ in energy, which is the reason for the misidentification of the doublet by Beutler & Guggenheimer (1934). Also, $5p^5 5d^2$ lies low in energy, leading to a greater complexity at long wavelengths than in the p-subshell spectra of the other alkalis (cf. also the analysis of data of Peart & Dolder (1975) mentioned above).

Returning now to the Ba I spectrum, we concern ourselves with transitions lowest in energy

TABLE 5. COMPARISON BETWEEN EXPERIMENT AND THEORY FOR SOME OF THE LOWER 5p-EXCITED CONFIGURATIONS IN Ba I

(a) For 5p⁵ 5d 6s²

$\lambda/\text{\AA}$	$\nu_{\text{obs}}/\text{cm}^{-1}$	$\nu_{\text{calc}}/\text{cm}^{-1}$	diff.	assignment (upper level)
576.11	173 578	180 813	-7 235	¹ P ₁
617.80	161 864	159 579	2 285	³ D ₁
693.66	144 163	139 213	4 950	³ P ₁

An upward shift of 15 664 cm⁻¹ was introduced to bring the calculations of table 3 (c) into approximate agreement with experiment. The remaining discrepancies are attributable to the approximate nature of the calculations in the presence of ¹P₁ wavefunction expansion (see text).

(b) For 5p⁵ 6s² 6d

$\lambda/\text{\AA}$	$\nu_{\text{obs}}/\text{cm}^{-1}$	$\nu_{\text{calc}}/\text{cm}^{-1}$	diff.	assignment (upper level)
531.47	188 157	188 088	69	($\frac{1}{2} \frac{3}{2}$) ₁
575.27*	173 831	174 008	-177	($\frac{3}{2} \frac{5}{2}$) ₁
579.37	172 600	172 491	109	($\frac{3}{2} \frac{3}{2}$) ₁

An upward shift of 2842 cm⁻¹ was introduced to bring the calculations of table 3 (d) into approximate agreement with experiment.

* This transition coincides with no. 4 of channel *f*.

(c) Intermediate coupling calculation of $J = 1$ levels in 5p⁵ 5d³ from the parameter values in table 3 (b)

5d ³ 5p ⁵ designation	energy	total (² D) ¹ P content	energy (nearest observed intense transition)
(² D) ¹ P	193 058	82	193 207
(⁴ P) ³ S	189 991	2	188 157
(⁴ F) ³ D	185 345	11	—
(² P) ¹ P	183 994	29	—
(⁴ P) ³ P	172 385	2.5	173 578 or 172 600
(² D) ³ D	168 384	5	—
(² F) ³ D	165 631	0.9	161 864
(² P) ³ P	153 267	7.5	—
(² D) ¹ P	150 515	30	—
(² P) ³ D	149 613	0.2	149 443
(² D) ³ P	148 225	0.09	148 750
(⁴ P) ⁵ P	146 113	14	—
(² P) ³ S	143 433	5	143 411
(⁴ P) ³ D	141 549	0.08	141 556
(⁴ P) ³ P	139 494	1.5	139 726
(² D) ³ D	136 959	9	136 147
(² P) ³ P	133 739	0.17	132 651
(⁴ F) ⁵ F	128 489	0.3	127 501
(⁴ F) ⁵ D	124 791	0.006	—

The calculations show that, on purely energetic grounds, excitation to the 5p⁵ 5d³ configuration could account for many of the observed transitions, especially at longer wavelengths. The configuration 5p⁵ 5d³ is probably more significant in Ba I than the corresponding configurations in other alkaline earth elements, as it overlaps extensively in energy with 5p⁵ 5d 6s². The (²D) ¹P content may give some idea of relative intensities in the spectator model: 5p⁶ 6s² ¹S₀ → 5p⁵{(5d² ¹S₀) 5d ²D} ¹P but, with repeated terms involved, it is in fact the {(²D) ¹P + (³D) ¹P} content.

within each channel. Quantum defect plots of the kind used in approach (i) do not suffice to classify these transitions for the following reasons:

(a) The approach of quantum defect theory by which configuration space for the excited electron is divided into inner and outer regions ceases to be valid for penetrating orbits.

(b) The Pauli principle does not permit unambiguous correlation of the lowest series members with specific channels.

(c) The separations of the 5d series members are determined by electrostatic interactions which are either absent or possess very different magnitudes in the limit configurations.

(d) Potential barrier effects lead to large quantum defect anomalies for 5d members.

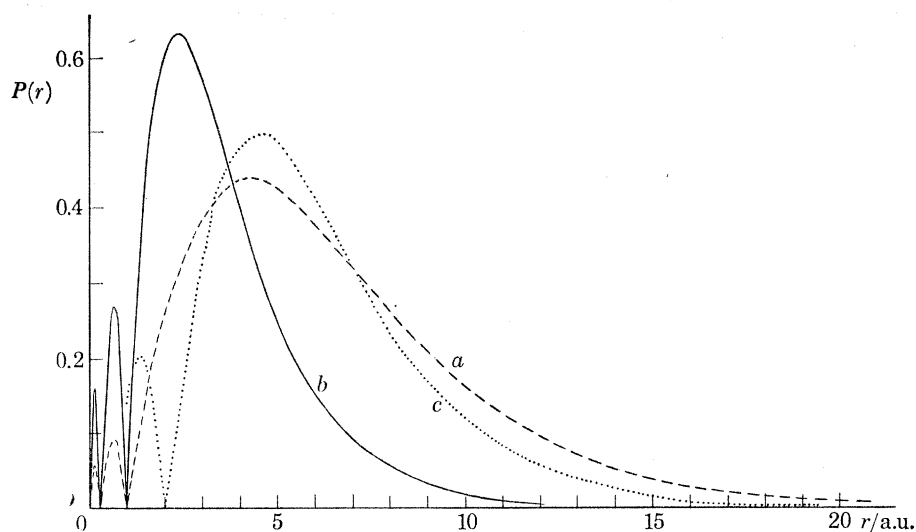
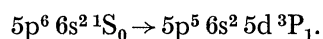


FIGURE 8. Expansion of the 5d wavefunction in Ba I $5p^5 6s^2 5d \ ^1P_1$ (a) compared with $5p^5 5d 6s^2$ configuration average (b) showing that the overlap of the 5d wavefunction with the 5p wavefunction for the ground state (c) is modified for the $^1S_0 \rightarrow ^1P_1$ transition. The modulus of the wavefunctions is plotted to show more clearly the extent of the overlap. Because of phase cancellation, the magnitude of the overlap is sensitive to small changes in the wavefunction and non-relativistic calculations cannot be expected to yield accurate values.

Nonetheless, certain low series members can be associated with channels in a plausible if ambiguous way, and they have therefore been included in tables 1 (a–l) with the reservation that this procedure may well be artificial in some cases.

When the lowest members are attached, there remains an important discrepancy, namely the line at 693.66 \AA ($144\,163 \text{ cm}^{-1}$) which is one of the most intense transitions in the spectrum but does not ‘fit’ clearly into any one of channels a–l.

A comparison between observed energies and the calculations of table 3 for the $5p^5 5d 6s^2$ and $5p^5 6s^2 6d$ configuration is made in table 5. This comparison suggests that, with arbitrary increases of $15\,664$ and 2842 cm^{-1} respectively in the value of E_{av} , the assignments deduced by approach (i) can be made consistent with the structure calculations, leading to the conclusion that the $144\,163 \text{ cm}^{-1}$ transition is



The percentage of 1P_1 in 3P_1 and 3D_1 , according to the calculation of table 3 (b) is significant. Also, the calculation is based on average of configuration parameters. When account is taken of the considerable wavefunction expansion of $5p^5 5d \ ^1P_1$ (see figure 8) it becomes clear that the intensity of the transition to 1P_1 will be affected and that the approximate calculation of table 3 (b)

does not suffice to determine relative intensities or even accurate energy intervals. This situation is similar to the one in Ca I (Mansfield & Newsom 1977) except that 1P_1 content of 3P_1 and 3D_1 in Ca I is very small.

Regarding the comparison between the r.p.a.e. predictions for Ba I (Wendin 1973 *a, b*, 1974) and experiment, the present data (figures 1, 2) suggest a strong similarity between the spectra of Cs I and Ba I and possibly also La I (figure 4) but that the spectra of Pr I–Yb I (figure 4) become gradually less affected by s–d mixing (Connerade & Tracy 1977). Similarly, the 4d spectrum of Ba I (Connerade & Mansfield 1974) shows modulations which are attributable to s–d mixing, whereas La I (Radtke, 1977 unpublished) and Eu I (Mansfield & Connerade 1976) both exhibit ‘clean’ profiles for the ‘giant resonance’. Comparisons between the r.p.a.e. calculations, which do not include the effect of s–d mixing, and experiment should be made for elements in which f.i.s.c.i. is not liable to cause a significant redistribution of oscillator strength.

4. CONCLUSION

New observations of the Ba I and Cs I spectrum have led to considerable extensions, and an empirical classification of the 5p spectrum of Ba I into series has been attempted. Comparisons with Hartree–Fock calculations and with the spectra of similar elements have enabled a preliminary analysis. Some revision of the interpretation of the lowest 5p-excited configurations in Cs I is suggested.

We thank Professor W. Mehlhorn and his collaborators of the University of Freiburg for communicating their data in advance of publication.

We thank Professor W. R. S. Garton, F.R.S., of the Blackett Laboratory, Imperial College and Professor W. Paul of the Physikalisches Institut Bonn for their continued interest and support.

Our thanks are extended to Herr K. Kueffner and our other colleagues of the Physikalisches Institut Bonn for assistance in operating the synchrotron radiation facility at the 500 MeV synchrotron. The present research has received financial support from the Science Research Council, the D.F.G., N.A.T.O. and E.S.R.O.

REFERENCES

- Armstrong, J. A., Esherick, P. & Wynne, J. J. 1977 *Phys. Rev. A* **15**, 180.
 Beutler, H. & Guggenheimer, K. 1934 *Z. Phys.* **88**, 25.
 Connerade, J. P. 1970 *a Astrophys. J.* **159**, 685.
 Connerade, J. P. 1970 *b Astrophys. J.* **159**, 695.
 Connerade, J. P., Garton, W. R. S., Mansfield, M. W. D. & Martin, M. A. P. 1976 *Proc. R. Soc. Lond. A* **350**, 47.
 Connerade, J. P., Garton, W. R. S., Mansfield, M. W. D. & Martin, M. A. P. 1977 *Proc. R. Soc. Lond. A* **357**, 499.
 Connerade, J. P. & Mansfield, M. W. D. 1974 *Proc. R. Soc. Lond. A* **341**, 267.
 Connerade, J. P., Mansfield, M. W. D., Thimm, K. & Tracy, D. H. 1974 *Proc. IVth Int. Conf. VUV Rad. Phys.*, pp. 99, 253. Vieweg-Pergamon.
 Connerade, J. P. & Tracy, D. H. 1977 *J. Phys. B (Lett.)* **10**, L235.
 Ederer, D. L., Lucatorto, T. B. & Saloman, E. D. 1974 *Proc. IVth Int. Conf. VUV Rad. Phys.* Vieweg-Pergamon.
 Ederer, D. L., Lucatorto, T. B., Saloman, E. D., Madden, R. P. & Sugar, J. 1975 *J. Phys. B* **8**, L21.
 Fliflet, A. W., Chase, R. L. & Kelly, H. P. 1974 *J. Phys. B* **7**, L443.
 Fliflet, A. W., Kelly, H. P. & Hansen, J. E. 1975 *J. Phys. B* **8**, L268.
 Garton, W. R. S., Connerade, J. P., Mansfield, M. W. D. & Wheaton, J. E. G. 1969 *Appl. Optics* **8**, 919.
 Griffin, D. C., Andrew, K. L. & Cowan, R. D. 1969 *Phys. Rev. A* **177**, 62.
 Hansen, J. E. 1974 *J. Phys. B* **7**, 1902.
 Hansen, J. E. 1975 *J. Phys. B* **8**, 2759.
 Hansen, J. E., Fliflet, A. W. & Kelly, H. P. 1975 *J. Phys. B* **8**, L127.

- Hellentin, P. 1976 *Physica scripta* **13**, 155.
- Lu, K. T. & Fano, U. 1970 *Phys. Rev. A* **2**, 81.
- Mansfield, M. W. D. 1973 *Astrophys. J.* **183**, 691.
- Mansfield, M. W. D. 1975 *Proc. R. Soc. Lond. A* **346**, 539.
- Mansfield, M. W. D. 1978 *Proc. R. Soc. Lond. A* **364**, 135.
- Mansfield, M. W. D. & Connerade, J. P. 1975 *Proc. R. Soc. Lond. A* **342**, 421.
- Mansfield, M. W. D. & Connerade, J. P. 1976 *Proc. R. Soc. Lond. A* **352**, 125.
- Mansfield, M. W. D. & Connerade, J. P. 1978 *Proc. R. Soc. Lond. A* **359**, 389.
- Mansfield, M. W. D. & Newsom, G. H. 1977 *Proc. R. Soc. Lond. A* **357**, 77.
- Mehlhorn, W., Breuckmann, B. & Hausmann, D. 1977 *Physica scripta* **16**, 177.
- Peart, B. & Dolder, K. T. 1975 *J. Phys. B* **8**, 56.
- Peart, B., Stevenson, J. G. & Dolder, K. T. 1973 *J. Phys. B* **6**, 146.
- Pejčev, V. & Ross, K. J. 1977 *J. Phys. B* **10**, 2935.
- Pejčev, V., Ottley, T. W., Rassi, D. & Ross, K. J. 1978 *J. Phys. B* **11**, 531.
- Rabe, P., Radler, K. & Wolff, H. W. 1974 *Vacuum ultraviolet radiation physics*, p. 247. Vieweg-Pergammon.
- Radtke, E. 1977 *Vth Int. Conf. VUV Rad. Phys.* (Proceedings unpublished.)
- Reader, J. 1976 *Phys. Rev. A* **13**, 507.
- Reader, J. & Epstein, G. L. 1973 *J. opt. Soc. Am.* **63**, 1153.
- Reader, J. & Epstein, G. L. 1975 *J. opt. Soc. Am.* **65**, 638.
- Roig, R. A. 1976 *J. opt. Soc. Am.* **66**, 1400.
- Rose, S. J., Pyper, N. C. & Grant, I. P. 1978 *J. Phys. B* **11**, 755.
- Schmitz, W., Breuckmann, B. & Mehlhorn, W. 1976 *J. Phys. B* **9**, L493.
- Süzer, S., Lee, S. T. & Shirley, D. A. 1976 *Phys. Rev. A* **13**, 1842.
- Tracy, D. H. 1977 *Proc. R. Soc. Lond. A* **357**, 485.
- Wendin, G. 1973a *Phys. Lett.* **46** A, 101.
- Wendin, G. 1973b *Phys. Lett.* **46** A, 119.
- Wendin, G. 1974 *Vacuum ultraviolet radiation physics*, p. 225. Vieweg-Pergammon.
- Wendin, G. 1976 *J. Phys. B* **9**, L297.

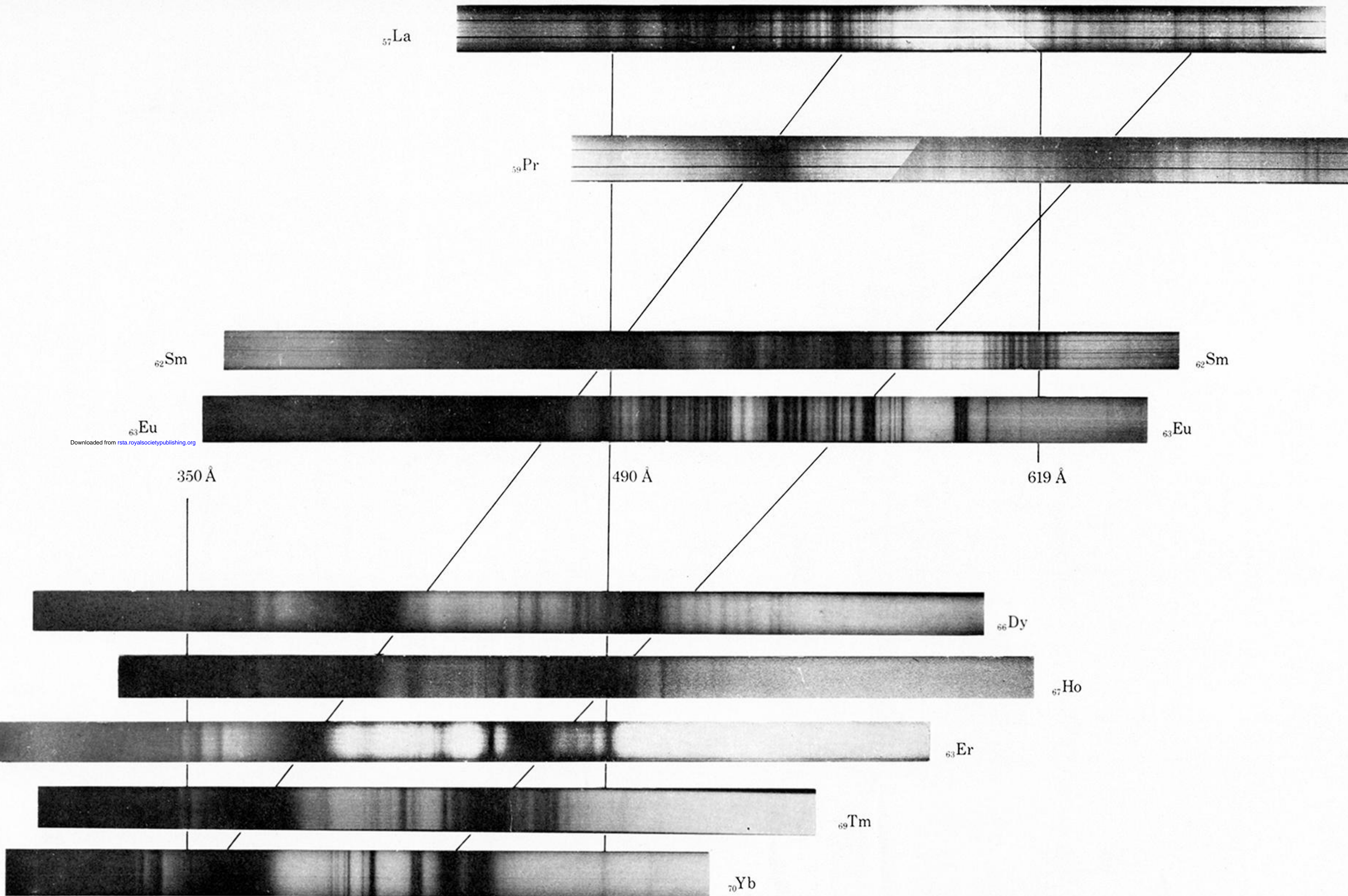


FIGURE 3. The 5p absorption spectra of the elements La I–Yb I recorded at the 500 MeV synchrotron in Bonn. The spectra of Sm I–Yb I have been reported by Tracy (1977) and work on La I–Pr I is still in progress. Note the persistence of the ^1P – ^3P limit structure from Yb back to Pr I. Around La I ($6s \times 5d$) mixing begins to complicate this pattern.

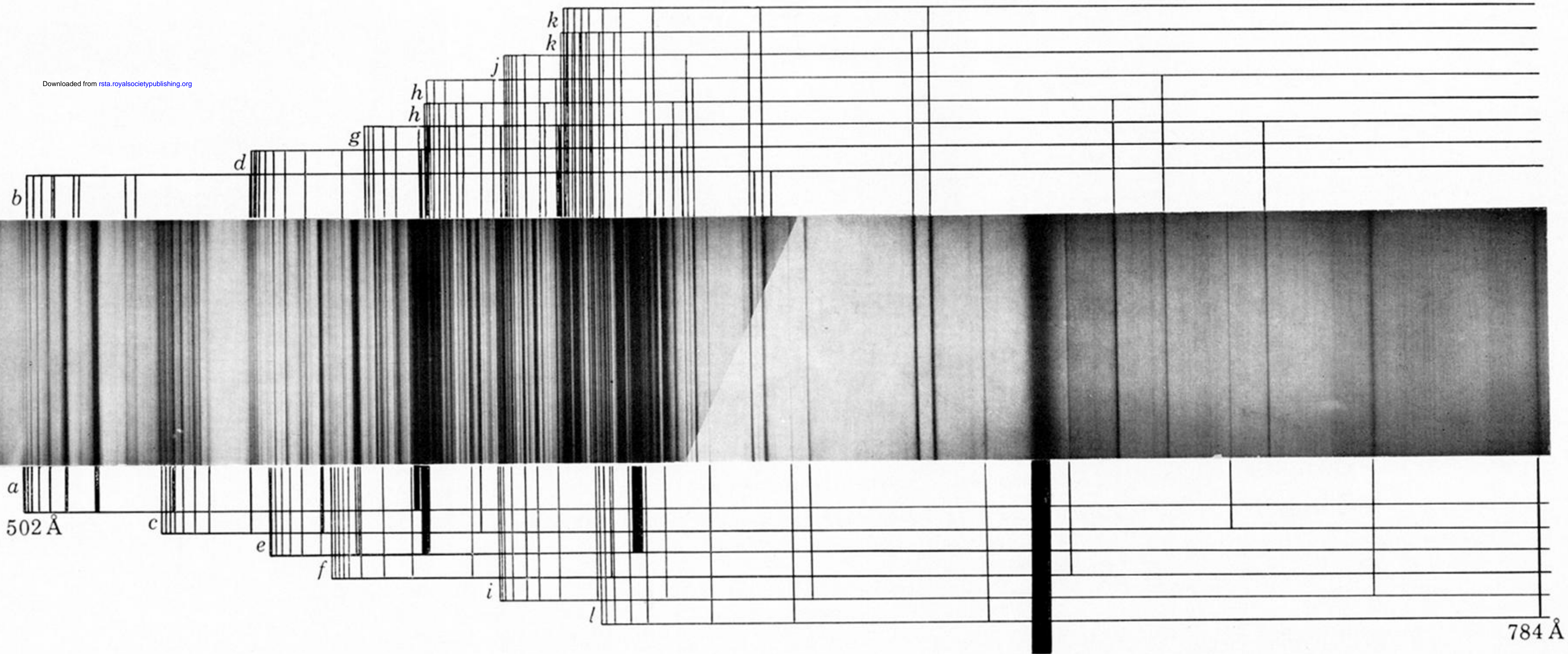


FIGURE 4. The 5p absorption spectrum of Ba I, showing how the ordering into 14 channels is accomplished (see text). The labels refer to tables 1 (*a-l*) and figure 6.